TRANSPORT PROPERTIES
OF GASEOUS AND ADSORBED
HELIUM

K. FOKKENS

TRANSPORT PROPERTIES OF GASEOUS AND
ADSORBED HELIUM

TRANSPORT PROPERTIES OF GASEOUS AND ADSORBED HELIUM

DOOR

KORNELIS FOKKENS

GEBOREN TE GRONINGEN IN 1937

Promotor:
PROF. DR K. W. TACONIS

Aan mijn ouders

Teneinde te voldoen aan het verzoek van de Faculteit der Wiskunde en Natuurwetenschappen volgt hier een overzicht van mijn studie.

Na beëindiging van mijn middelbare schoolopleiding aan het Gymnasium Haganum te 's-Gravenhage met het afleggen van het eindexamen Gymnasium β in 1955, begon ik mijn studie in de natuurkunde aan de Rijksuniversiteit te Leiden. In 1958 legde ik het candidaats A' af. Vervolgens deed in ik 1961 het doctoraal examen experimentele natuurkunde (na hiertoe de vereiste tentamina te hebben afgelegd). Sedert september 1958 ben ik werkzaam in het Kamerlingh Onnes Laboratorium als medewerker van de helium werkgroep onder leiding van Prof. Dr K. W. Taconis. Aanvankelijk assisteerde ik Dr C. J. N. van den Meijdenberg bij metingen en berekeningen over de invloed van ^{3}He op filmtransport, daarna werkte ik bij Dr F. A. Staas aan metingen van de viscositeit van vloeibare ^{3}He–^{4}He mengsels en onderzoekingen betreffende laminaire en turbulente stroming van ^{4}He door wijde capillairen. Medio 1960 begon ik een onderzoek over de warmtegeleiding van vloeibare ^{3}He–^{4}He mengsels beneden $1°$K. In 1961 werd een begin gemaakt met de in dit proefschrift vermelde experimenten. De metingen werden verricht met achtereenvolgens de assistentie van de heren J. Walter, H. Albas en W. M. van Alphen en van mej. W. Vermeer. De discussie vond plaats in samenwerking met Dr R. de Bruyn Ouboter. De gewaardeerde technische assistentie werd vooral verleend door de heren E. S. Prins en J. P. Hemerik die de gebruikte apparaten hebben geconstrueerd en door de heren L. Neuteboom en J. Turenhout, die het cryogene deel verzorgden.

Dr W. I. Honeywell en Dr T. W. Adiar ben ik dank verschuldigd voor het corrigeren van het Engels.

Sinds 1959 heb ik geassisteerd op het practicum voor prae-candidaten. In 1966 heb ik het werkcollege verzorgd behorende bij het natuurkunde college van Dr C. J. N. van den Meijdenberg voor eerstejaars chemici.

In 1961 ben ik als wetenschappelijk medewerker in dienst getreden van de Stichting voor Fundamenteel Onderzoek der Materie (F.O.M.).

CONTENTS

INTRODUCTION

During the last twenty years much work has been done to calculate the transport properties of gases at such low temperatures, that quantum effects arise, caused by the increase of the De Broglie wavelength and by symmetry properties.

Experimental data below 1.3°K, however, were not yet available. Therefore we set up an experiment to measure the heat conductivity coefficient of ^{3}He and ^{4}He in this temperature region that could be controlled by means of a cryostat cooled with ^{3}He. These investigations are described in chapter I. Although the pressure of the gas was always so low, that no bulk liquid condensation could occur yet an unsaturated multilayer film was adsorbed. In the case of ^{4}He the appearance of this film with its superfluid properties, when the thickness came above a critical value, caused difficulties by its indirect contribution to the heat conductivity. This fact made it necessary to study the onset of superfluidity in unsaturated ^{4}He films and some ^{3}He–^{4}He mixtures, as experimental data below 1.3°K were not yet available for ^{4}He and not at all for the mixtures. These experiments are described in chapter II. Whereas for bulk helium the onset of superfluidity coincides with the peak in the specific heat at the λ-point, this is not the case for unsaturated films as is again confirmed by our results. Not only the onset but also the destruction of superfluidity, when the film has reached its critical velocity, was examined. At supercritical velocities the flim flows not frictionless any more, but under the influence of a gradient in the chemical potential the velocity can still increase somewhat as follows from our data.

In heat conduction measurements of liquid helium always a temperature jump between the wall and the liquid is included, if the temperatures of the walls are measured instead of the temperature of the helium. This effect is called the Kapitza resistance. This was also the case with the films we examined. The Kapitza resistance was measured as a function of the thickness of the films and of the temperature. As its value was independent of the thickness we conclude that the resistance is situated between the wall and the first adsorbed layer.

THE HEAT CONDUCTIVITY OF ³He
AND ⁴He AND THEIR MIXTURES IN THE GASEOUS STATE
BETWEEN 0.5 AND 3°K

Synopsis

The heat conductivity coefficient of gaseous ³He, ⁴He and a 50% ³He–⁴He mixture is measured between 0.5°K and 3°K. The apparatus consists of two parallel horizontal plates, and a shield ring around the upper one. The distance between the plates is variable. A discussion about several methods to measure the heat conductivity is included. Our results are compared with theoretical calculations of the transport properties of the helium isotopes by De Boer, Keller, Buckingham and Scriven. In general a satisfactory agreement is found.

1. *Introduction.* It is interesting to investigate the transport properties of gases at low temperatures, because quantum effects clearly appear here. As soon as the de Broglie wavelength of relative motion is comparable with the molecular diameter, diffraction effects cause quantum mechanical deviations from the classical behaviour. Also when this de Broglie wavelength is of the order of the mean free path, symmetry effects can appear due to the overlapping of the wave functions. In our experiment this is not important, since there the de Broglie wavelength is at least still a factor of 100 smaller then the mean free path. However because of the fact, that at the collision of two identical particles the wave functions must be symmetrised, the collision cross-sections and therefore the transport properties depend on the statistics which the particles obey.

The gases we investigated were ³He and ⁴He. These elements are very appropriate for these experiments, because at very low temperatures they do not condense at pressures high enough to measure the transport properties in a region where they are independent of the pressure. As ³He consists of an odd number of particles and ⁴He of an even number, the two gases obey different statistics, which will cause a sizeable difference in heat conduction. With this in mind several authors have made theoretical calculations of the transport properties of ³He and ⁴He. In chronological sequence they are Buckingham, Hamilton and Massey[1] De Boer[2][3],

1

Cohen[4]), Buckingham and Scriven[5]), and Keller[6]). Buckingham e.a., used an intermolecular potential with an exponential repulsion and an attractive field, consisting of an inverse sixth and eighth power term, while De Boer and Cohen used a Lennard-Jones type potential, as also did Keller. In the case of ^{4}He the latter found about the same values as De Boer, but for ^{3}He a rather large difference appeared. The values of Keller are more preferable, because of the higher accuracy he could obtain by using an electronic computer. Buckingham calculated the transport properties in the first Enskog approximation. Keller calculated also the second approximation, as also did De Boer for ^{4}He below 1.6°K. It appears that in the first approximation the influence of the potential field is not very large.

Measurements of the heat conductivity coefficient have been performed by Ubbink[7]), who investigated ^{4}He, and by Challis[8]), who studied both gases. Viscosity measurements of ^{4}He have been done by Van Itterbeek and Keesom[14]), Van Itterbeek, Schapink, Van den Berg and Van Beek[9]), and Becker, Misenta and Schmeissner[10]). The latter have also investigated ^{3}He and some mixtures of ^{3}He and ^{4}He. All these experiments were limited to the temperature region above 1.3°K.

By means of a ^{3}He-cryostat we were able to measure the heat conductivity coefficient at lower temperatures. For ^{3}He we extended the region of measurement to 0.5°K and for ^{4}He to 0.9°K. The former limit was caused by the operating characteristics of the ^{3}He-cryostat, the latter by the fact that the vapour pressure of ^{4}He below 0.9°K is so low, that Knudsen effects appear. Finally we also made some preliminary measurements with a 50% ^{3}He–^{4}He mixture.

2. *The method.* The heat conductivity coefficient, λ, is defined by the general heat conduction equation

$$J = -\lambda \, \text{grad} \, T$$

where J is the heat current density and T the temperature. If the temperature gradient is only in one direction, then

$$J_x = -\lambda (\mathrm{d}T/\mathrm{d}x),$$

and if λ is a linear function of T in the temperature region ΔT where ΔT must be small with respect to T, we have

$$J_x = -\lambda (\Delta T/\Delta x).$$

The total heat current through a surface A normal to J is

$$JA = \dot{Q} = -\lambda A (\Delta T/\Delta x),$$

$\Delta x/\lambda A$ is called the heat resistance R, and

$$\Delta T = R\dot{Q}.$$

2

This formula is analogous to Ohm's law for an electric circuit. To calculate λ the following quantities must be measured:

1) The total heat current $\dot{Q}$.
2) The temperature difference ΔT.
3) The factors A and Δx.

For stationary measurements of the heat conductivity coefficient there are two methods: the wire method and the plate method. An apparatus according to the wire method consists of a wire W at the axis of a cylinder c (fig. 1). A known current through the wire causes the desired amount of
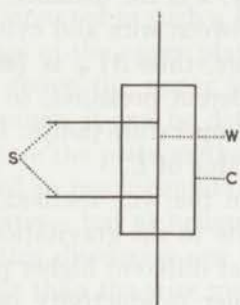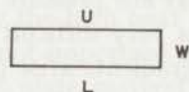
Fig. 1. Wire method.   Fig. 2. Plate method.

Joule heating, and by measuring the resistance of the wire its temperature is determined. The cylinder wall is kept at a constant temperature. A plate-method apparatus consists of two parallel horizontal plates (fig. 2) of which the upper one u is heated and the lower one l kept at a constant temperature. During a long time the wire method was considered as the best one for heat conduction experiments, but it has some important disadvantages that can be avoided if one uses the plate method in a correct way. The disturbing effects in both methods are

a) The amount of heat, that flows away through the frame of the apparatus and not through the gas.
b) The temperature jumps between the gas and the wall.
c) The amount of heat transported by convection.
   These effects will be discussed for both methods.

The wire method. a) When heat is supplied to the wire, part of it is carried off by the wire itself. If the heat conductivity of the wire is known, one can calculate this quantity in principle, but end effects make this rather difficult. To eliminate these, Weber used contacts s attached to the wire to measure the potential difference over that part of the wire along which no temperature gradient was present. (fig. 1).

b) If the energy exchange between gas molecules and the wall is not complete at a collision, a temperature jump between the gas and the wall

3

arises. Knudsen defined an accomodation coefficient

$$a = (E_1 - E_2)/(E_1' - E_2),$$

where E_1, E_1' and E_2 are the mean energies of the gas molecules, respectively after collision with the wall as it happens in reality, after collision with the wall with complete energy exchange, and before collision with the wall. Smoluchowski found for the temperature jump at the wall the formula, $\Delta T_w = (-15/2\pi)(2 - a)/2a) L \, \partial T/\partial x = -\gamma(\partial T/\partial x)_w$, where L is the mean free path and $(\partial T/\partial x)_w$ is the temperature gradient in the gas near the wall.

In the wire apparatus $\partial T/\partial x = -\Delta T/x \ln(R/r)$, where R and r are the radius of the cylinder and the wire respectively, x is the distance from the wire, and ΔT is the temperature difference between wire and cylinder. At small x the temperature gradient becomes large, thus ΔT_w is large. One can correct for this effect by measuring at different pressures, so that the mean free path changes. So one gets different temperature jumps. This must be done at low pressure to get a rather large value of L.

c) It is very difficult to avoid convection in the wire method, because density gradients arise perpendicular or opposite to the gravitational field. One can try to correct for it by measurements at different higher pressures, but it is difficult to separate between a higher conductivity caused by convection or by a real pressure dependence, and in fact here one is confronted with the most important disadvantage of the wire method.

The plate method. a) Part of the heat supplied to the upper plate u (fig. 2) will be conducted through the wall w to the lower plate l. There will not be such a heat flow, if a part of the wall is at the same temperature as the upper plate. This can be achieved by using a shield ring around the upper plate, which is connected with l by the wall w_1 and with u by w_2
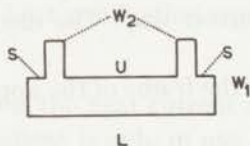
Fig. 3. Plate method with shield ring.   Fig. 4. Plate method with shield plate.
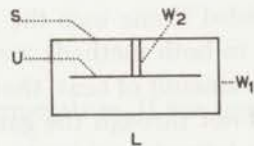
(fig. 3). This shield ring is heated till it has the temperature of u. In that case all heat supplied to the upper plate will go through the gas to the lower plate in a parallel pattern. One can also try a shield plate above the upper plate (fig. 4) like Ubbink[7] did, but this construction is more likely to induce convection.

b) The temperature gradient between two parallel plates is the same everywhere if the heat conductivity coefficient is constant. Therefore temperature jumps at the wall are much smaller than in the wire apparatus

with the same temperature difference across the gas. As will be shown a temperature jump is equivalent to an extra heat resistance, which in the first approximation is independent of the resistance between the plates. One can eliminate this effect by varying the distance. Then the variation in heat resistance is only caused by the variation of the distance across the gas.

c) The plate method is very suitable for avoiding and for detecting convection. If the upper plate is warmer than the lower one, a density gradient in the direction of the gravitational field is established. In this case there will be no convection. Only corner effects may remain where the upper plate meets the wall. These are avoided by the shield ring around the upper plate, which is mounted in such a way that no sharp temperature gradients occur at the edge of the upper plate. This is not the case when the shield plate is situated above the upper plate. Since convection grows with increasing plate distance, it can be detected by varying the plate distance. At room temperature the plate method has the disadvantage of the long times, that are needed to reach equilibrium – this is caused by the high heat capacity of the plates – but at helium temperatures this is not important anymore.

From this discussion one can conclude that the plate method is more favourable than the wire method. Therefore, we constructed an apparatus consisting of two plates and a shield ring with a mechanism to vary the distance between the plates. The following formalism can be set up to describe the heat currents in this plate apparatus.

We define the quantities:

$\dot{Q}_u$ as the amount of heat supplied per second to the upper plate.

$\dot{Q}_u^I$ as the part of $\dot{Q}_u$, that is transported through the gas to the lower plate.

$\dot{Q}_u^{II}$ as the part of $\dot{Q}_u$ that is transported along the wall and via the shield ring.

$\dot{Q}_s$ as the amount of heat supplied per second to the shield ring.

$\dot{Q}_s^I$ as the part of $\dot{Q}_s$ that flows to the lower plate.

$\dot{Q}_s^{II}$ as the part of $\dot{Q}_s$ that flows to the upper plate.

R_1, R_2 and R_3 are the heat resistances respectively between: upper and lower plate, upper plate and shield ring, and shield ring and lower plate.

T_u, T_s and T_l are the respective temperatures of the upper plate, shield ring and lower plate.

As has already been shown a heat conduction apparatus can be described analogous to an electric circuit, where ΔT corresponds to the potential difference, R to the resistance, and $\dot{Q}$ to the current. A diagram of the circuit is shown in fig. 5. It is possible, using Ohm's law and Kirchhoff's law, to calculate the temperatures T_u and T_s as a function of the heat currents $\dot{Q}_u$ and $\dot{Q}_s$. If only the heat input $\dot{Q}_u$ is used, then $T_u - T_l = \dot{Q}_u R$ where R

5
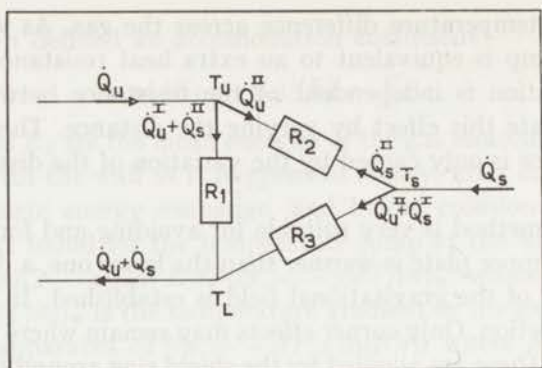
Fig. 5. Electrical analogon of the heat conduction cell.

is the substitution resistance defined as $1/R = 1/R_1 + 1/(R_2 + R_3)$. From this it follows:

$$(T_u - T_l)_{\dot{Q}_s=0} \atop \dot{Q}_u = \frac{R_1(R_2 + R_3)}{R_1 + R_2 + R_3} \dot{Q}_u.$$

The rise of T_l caused by $\dot{Q}_s$ is calculated in the following way:

$$\left. \begin{array}{l} (T_s - T_l)_{\dot{Q}_u} = \dot{Q}_s^{\mathrm{I}} R_3 = \dot{Q}_s^{\mathrm{II}}(R_1 + R_2) \\ \dot{Q}_s^{\mathrm{I}} + \dot{Q}_s^{\mathrm{II}} = \dot{Q}_s \end{array} \right\} \dot{Q}_s^{\mathrm{II}} = \frac{R_3}{R_1 + R_2 + R_3} \dot{Q}_s.$$

The current $\dot{Q}_s^{\mathrm{II}}$ flows through R_1, so

$$(T_u - T_l)_{\dot{Q}_s \atop \dot{Q}_u=0} = R_1 \dot{Q}_s^{\mathrm{II}} = \frac{R_1 R_3}{R_1 + R_2 + R_3} \dot{Q}_s.$$

The total temperature difference

$$T_u - T_l = \frac{R_1(R_2 + R_3)}{R_1 + R_2 + R_3} \dot{Q}_u + \frac{R_1 R_3}{R_1 + R_2 + R_3} \dot{Q}_s. \tag{1}$$

In the same way the temperature $T_s - T_l$ can be calculated.

$$T_s - T_l = \frac{R_3(R_1 + R_2)}{R_1 + R_2 + R_3} \dot{Q}_s + \frac{R_1 R_2}{R_1 + R_2 + R_3} \dot{Q}_u. \tag{2}$$

From (1) and (2), it follows that if $T_u - T_s = 0$,

$$T_u - T_l = \dot{Q}_u R_1. \tag{3}$$

In that case all heat supplied to the upper plate will be transported through the gas between both plates. From (1) and (2) it can also be concluded that, if R_1, R_2 and R_3 are independent of the heat currents, T_u and T_s are linear functions of $\dot{Q}_u$ and $\dot{Q}_s$.

During the measurements it is impossible to realise exactly the state, where

T_u equals T_s, because of the use of nonidentical carbon thermometers, for which the complete calibration curve could only be calculated after the measurements. We used a graphical method to accomplish this. While $\dot{Q}_u$ is kept constant, T_u and T_s are measured at different values of $\dot{Q}_s$. On a graph one gets now two straight lines, $T_u(\dot{Q}_s)$ and $T_s(\dot{Q}_s)$. At the point of intersection T_u equals T_s.

The heat that is supplied by the heater to the upper plate is called $\dot{Q}_u$. This is a known quantity. However, when the outer He bath is warmer there is always a small unknown heat leak from the outer He bath to the upper plate and the shield ring. This quantity is called $\dot{Q}_0$. One must make a correction for this, and also for the temperature jump. With respect to these corrections one can write:

$$T_u - T_l = \Delta T = (\dot{Q}_u + \dot{Q}_0) R_1 = (\dot{Q}_u + \dot{Q}_0)(R_g + R_w) = \Delta T_g + \Delta T_w \quad (4)$$

where ΔT_g is the temperature difference across the gas layer,

ΔT_w is the temperature jump at the wall,

R_g is the resistance of the gas layer,

R_w is the transition resistance at the wall.

Differentiating (4) with respect to $\dot{Q}_u$ gives

$$\partial \Delta T / \partial \dot{Q}_u = R_g + R_w, \quad (5)$$

because $\dot{Q}_0$ is independent of $\dot{Q}_u$; and, further,

$$\frac{\partial(\partial \Delta T / \partial \dot{Q}_u)}{\partial h} = \frac{\partial R_g}{\partial h}, \quad (6)$$

if R_w is independent of h, where h is the distance between the plates.

Previously we defined $R = \Delta x / \lambda A$ as the resistance of the gas between the plates with separation Δx and surface area A. Therefore $R_g = h/A\lambda$. Differentiating with respect to h gives

$$\partial R_g / \partial h = 1/A\lambda. \quad (7)$$

From (5) it follows that, in order to correct for $\dot{Q}_0$, ΔT must be measured as a function of $\dot{Q}_u$.

For different $\dot{Q}_u$, T_u and T_s are measured as a function of $\dot{Q}_s$. Thus one gets several sets of two straight lines. If R_1, R_2 and R_3 are independent of $\dot{Q}_u$, the slopes of these lines are equal. This fact enables a more accurate determination of the lines, and therefore of the intersection points. It follows from (6) that it is essential to measure at different plate distances. First ΔT is determined as a function of $\dot{Q}_u$ for some values of h. The slope of these straight lines, $\partial \Delta T / \partial \dot{Q}_u$, is then plotted as a function of h. The slope of this line gives $1/A\lambda$, from which λ can be derived. This method is only correct if R_w is independent of h, or in others words, if R_w is independent

7

of T.

$$R_w = \frac{\Delta T_w}{\dot{Q}_u} = \frac{-\gamma(\partial T/\partial x)}{-\lambda A(\partial T/\partial x)} = \frac{\gamma}{\lambda A}. \tag{8}$$

R_w depends on the temperature via γ and λ, where λ is the most important factor. If λ changes strongly within the temperature region ΔT, this gives a different R_w at the upper and the lower plate, and also a change in R_1. In both cases this influence works in the same direction, namely a bending of the line $\Delta T(\dot{Q}_u)$. The effects, however, cannot be separated. We have found that within our accuracy $\Delta T(\dot{Q}_u)$ is always a straight line, so that we can apply the method we developed to calculate λ.

3. *The apparatus* (fig. 6). The heat conduction cell in the apparatus consists of the upper plate u and the lower plate l, both made of copper. The surface area of u is 3.46 cm² at room temperature. A cavity b is drilled in l, in which the cooling liquid is condensed. In the temperature range below 1.3°K this is ³He; above 1.3°K ⁴He is used. The vapour can be pumped off through tube p, in order to lower the temperature. A copper shield ring s is mounted around u. It is connected to u by the stainless steel cylinder w_1, which has a wall thickness of 5×10^{-3} cm, and to l by successively the stainless steel bellows a and another thin stainless steel cylinder w_2. Inside w_2 is a cylinder i made of celleron. This cylinder isolates w_2 from the gas between the plates.

In order to vary the distance between u and l, the following construction was made. The bellows f, which can be compressed or stretched by means of a micrometer system, are soldered on the top of the vacuum jacket v. The micrometer system consists of the screws e and h which have a difference in speed of 0.25 mm. The screw e is mounted on the vacuum jacket, h on the top of the bellows f. The displacement can be read on the scale g. This motion is transmitted to the system of the upper plate and the shield ring by means of the wire w. In this way the upper plate and the shield ring can be moved up and down with respect to the lower plate, which is rigidly connected to the vacuum jacket via p and via the thin walled stainless steel tube n. This tube connects l to a rigid frame work consisting of three supports r which lead to a separate extra bottom plate t. The entire frame is fastened inside the top plate of the vacuum jacket.

The vacuum jacket itself encloses the whole system and can easily be removed, while the apparatus remains supported. One turn of the micrometer gives 0.25 mm change in plate distance at room temperature. At the operating temperature we must correct for the shrinkage of e and h. This correction must also be applied to the surface area of u.

The gas is introduced between the plates through the capillary c with 1.8×10^{-2} cm inner diameter. Outside the vacuum jacket it widens to a
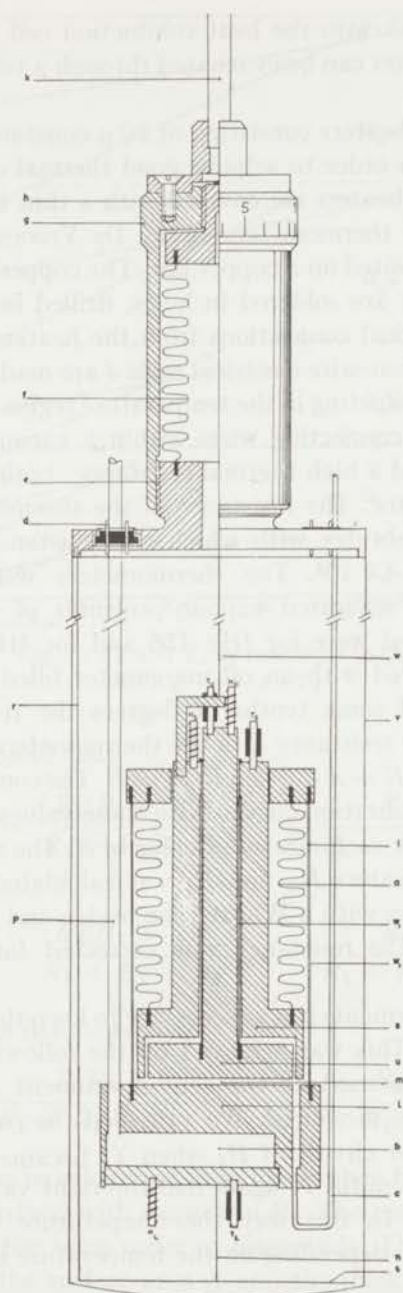
Fig. 6. The apparatus.

tube with 0.4 cm inner diameter enabling the evacuation of the apparatus in a short time, and a quick establishing of the pressure equilibrium during the measurements. Inside the vacuum jacket the capillary must be narrow

to reduce the heat leak into the heat conduction cell from the outer ^{4}He bath. The vacuum jacket can be evacuated through a tube that is not shown in fig. 6.

H_u, H_s and H_l are heaters consisting of 50 μ constantan wire, wound on a small copper bar. In order to achieve good thermal contact between the wire and the bar, the heaters are covered with a thin layer of lacquer. T_u, T_s and T_l are carbon thermometers of the De Vroomen type in which a layer of carbon is deposited on a copper bar. The copper bars for the heaters and the thermometers are soldered in holes, drilled in the plates and the shield ring. The electrical connections from the heaters and thermometers to the vacuum tight, four-wire electrical seals d are made from thin niobium wire, which is superconducting in the temperature region where we measured. The requirements for connecting wires within a vacuum jacket are a low electrical resistance and a high thermal resistance; both are fullfilled in the case of a superconductor. The resistance of the thermometers is measured with a dc Wheatstonebridge with which the resistance can be measured with an accuracy of 1 : 10^4. The thermometers were calibrated from measurements of the saturated vapour pressures of ^{3}He and ^{4}He. The temperature scales used were for ^{4}He T58 and for ^{3}He T62. The vapour pressures were measured with an oil manometer filled with Octoil-S. For temperature ranges of some tenths of degrees the relation between the temperature T and the resistance R of the thermometers could be described with the formula $^{10}\log R = A\sqrt{(^{10}\log R/T)} + B$. The constants A and B were calculated from the calibration curve. With these values the proper temperature was calculated for each measured value of R. The amount of heat that was supplied to the heaters H_u and H_l was calculated by measuring the resistance of the heaters with a Wheatstone bridge and reading the current on a milliampmeter. The resistance was corrected for the resistance of the connecting wires.

For accurate measurements it was necessary to keep the temperature of the lower plate constant. This was achieved by the following mechanism. An electronic recorder was used as the zero instrument in the Wheatstone bridge with which T_l is measured. We provided the recorder with a relay which closed the heater circuit of H_l when T_l became too low. Then the lower plate was heated untill T_l again had the right value, and the heater circuit was reopened. In this way the temperature was kept constant within 10^{-4} to 10^{-5} °K, depending on the temperature region.

4. *Results*. The results of the measurements are illustrated in the figures.

a) ^{3}He. Fig. 7 gives an example of the behaviour of T_u and T_s as a function of $\dot{Q}_s$ for various values of $\dot{Q}_u$. We see, that a linear dependence exists, and that the slope of the straight lines is independent of $\dot{Q}_u$. This proves that R_1, R_2 and R_3 are independent of $\dot{Q}_u$ and $\dot{Q}_s$.
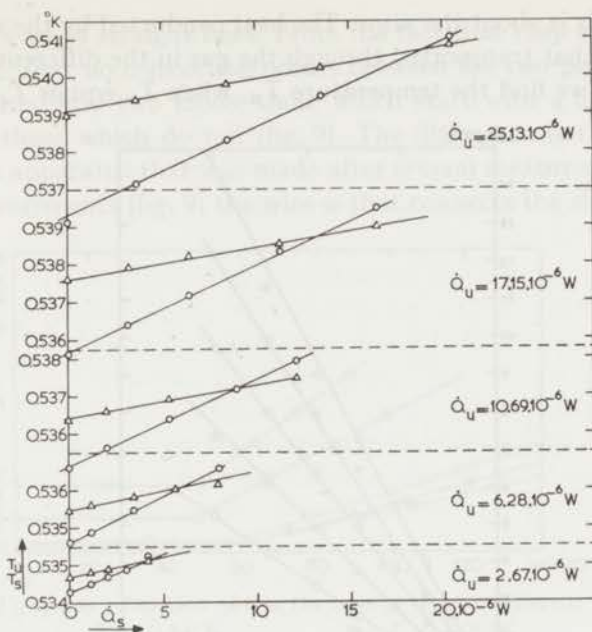
Fig. 7. T_u and T_s as functions of $\dot{Q}_u$.

○: T_u △: T_s

In section 2 we found that

$$T_u - T_l = \frac{R_1(R_2 + R_3)}{R_1 + R_2 + R_3}\,\dot{Q}_u + \frac{R_1 R_3}{R_1 + R_2 + R_3}\,\dot{Q}_s$$

and that

$$T_s - T_l = \frac{R_3(R_1 + R_2)}{R_1 + R_2 + R_3}\,\dot{Q}_s + \frac{R_1 R_3}{R_1 + R_2 + R_3}\,\dot{Q}_u.$$

From these formulas it follows that

$$\frac{\partial T_u}{\partial \dot{Q}_s} = \frac{R_1 R_3}{R_1 + R_2 + R_3} \quad \text{and} \quad \frac{\partial T_s}{\partial \dot{Q}_s} = \frac{R_3(R_1 + R_2)}{R_1 + R_2 + R_3}.$$

These derivatives can be calculated from fig. 7. Then from the two equations, R_2 and R_3 can be derived with respect to R_1. The result is, that R_1, R_2 and R_3 appear to be of the same order of magnitude. This can be understood, when one observes the surface area A and the thickness Δx across the gas in the areas between u, s and l. The surface of the area between u and l is 3.46 cm² and the thickness varies from 0.1 to 1 mm. Between u and s is an area with a surface of 6 cm² and a thickness of about 1 mm. The area between the shield ring and the lower plate, has a surface and a thickness of the same order of magnitude. The ratio $\Delta x/A$ is important for R. In all

11

three cases, this is about the same. The heat conducted by the walls is much smaller, than that transported through the gas in the different areas.

From fig. 7 we find the temperature T_u, when T_u equals T_s.
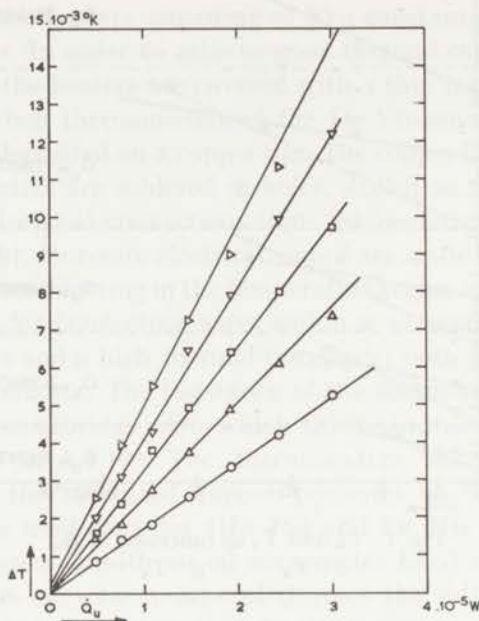
Fig. 8. ΔT as a function of $\dot{Q}_u$ for different values of h.

In fig. 8 the temperature difference $T_u - T_l$ is plotted as function of $\dot{Q}_u$ for the various values of h. We observe that the dependence is again linear. It also appears that the lines intersect the $\dot{Q}_u$ axis at a negative value of $\dot{Q}_u$. It is negative because of the heat leak $\dot{Q}_0$, which is about 10^{-6} W.

The slope of the lines gives $\partial \Delta T / \partial \dot{Q}_u$ for different plate distances. These are plotted in fig. 9 and 10 for all temperatures at which we measured. Here
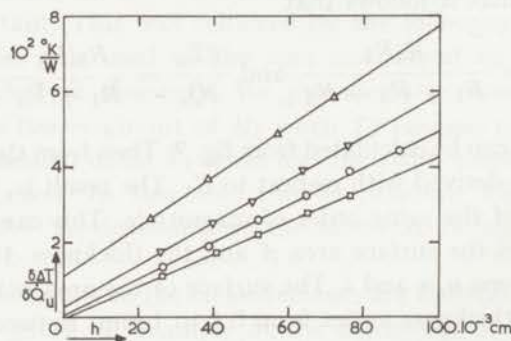
Fig. 9. $\partial(\Delta T)/\partial \dot{Q}_u$ as a function of h in the case of ^{3}He for different temperatures.

$\triangle: T = 0.65°$K $\circ: T = 0.90°$K

$\triangledown: T = 0.77°$K $\square: T = 1.086°$K

again we get a set of straight lines. From the fact that they are straight we may conclude, that no convection occurs between the two plates. The lines can be separated into two kinds, those which start with a horizontal part (fig. 10) and those which do not (fig. 9). The difference is the result of a change in the apparatus that was made after several measurements. During the first measurements (fig. 9) the wire w that connects the shield ring with
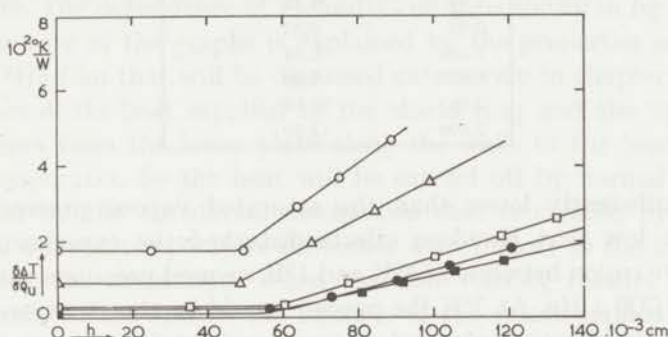
Fig. 10. $\partial(\Delta T)/\partial \dot{Q}_u$ as a function of h in the case of ^{3}He for different temperatures.

$\bigcirc: T = 0.54°$K $\bullet: T = 2.06°$K

$\triangle: T = 0.82°$K $\blacksquare: T = 3.099°$K

$\square: T = 1.607°$K

the upper bellows was so long that when the micrometer was turned to its lowest point, both plates touched each other. Turning the micrometer upwards immediately effected a displacement of the upper plate. After some measurements it appeared that the connection between wire and shield ring was not strong enough. Then a better one was made, but now the wire was about 0.5 mm longer, so that only after about two turns of the micrometer the upper plate was raised. Since it was difficult to detect this point exactly, we decided to take h as the displacement of the micrometer. It is not the plate distance. For this reason $\partial \Delta T/\partial \dot{Q}_u$ was a constant till h became so large that the upper plate was raised. The value of this constant part will be discussed later. The slope of the h dependent part is

$$\frac{\partial(\partial \Delta T/\partial \dot{Q}_u)}{\partial h} = \frac{1}{A\lambda'} \quad \text{or} \quad \lambda' = \frac{1}{A \dfrac{\partial(\partial \Delta T/\partial \dot{Q}_u)}{\partial h}}.$$

In this relation λ' is the value of the heat conductivity coefficient, we should get using the room temperature values of A and h. In order to correct for the shrinkage that occurs, we must multiply λ' with the factor 1.0027. Thus $\lambda = 1.0027 \, \lambda'$. The final values are tabulated in table I.

In these measurements of the heat conductivity coefficient one is restricted to a rather small pressure range. It was necessary to work at a

13

TABLE I

The heat conductivity coefficient λ for ^{3}He gas	
$T(^\circ K)$	$\lambda(W/^\circ Kcm)$
0.54	4.07×10^{-5}
0.65	4.48
0.77	5.14
0.82	5.45
0.90	5.87
1.086	6.84
1.607	9.20
2.06	10.68
3.099	12.50

pressure sufficiently lower than the saturated vapour pressure of ^{3}He, but not so low that Knudsen effects disturbed the experiment. In the temperature region between 0.54°K and 1°K we used pressures varying from 60 μ Hg to 200 μ Hg. At 3°K the pressure could be chosen at several millimeters Hg. We always performed measurements at different pressures, and were satisfied to find the same value of the heat conductivity coefficient.

b) ^{4}He. Generally the behaviour of the heat currents as a function of temperature was the same at the ^{4}He as at the ^{3}He measurements, which
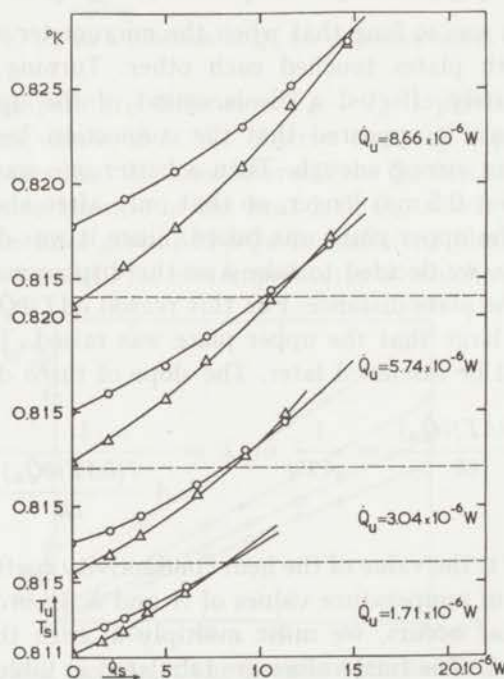
Fig. 11. T_u and T_s as function of Q_s, in the case of ^{4}He, with a superfluid film.
o: T_u $\triangle$: T_s

means that T_u and T_s depended linearly on $\dot{Q}_s$. An important exception, however, was observed in those experiments, where a superfluid unsaturated ⁴He film was adsorbed on the walls of the apparatus. This phenomenon occured at the lowest temperatures, where we were obliged to work at a rather high value of P/P_0 in order to avoid mean free path effects. P is the pressure of the gas and P_0 the saturated vapour pressure at the operating temperature. The dependence of T_u and T_s on $\dot{Q}_s$ is shown in fig. 11.

The curvature of the graphs is explained by the properties of a mobile superfluid ⁴He film that will be discussed extensively in chapter II. Under the influence of the heat supplied to the shield ring and the upper plate the film flows from the lower plate along the walls to the heated plates, where it evaporates. So the heat will be carried off by normal heat conduction and by the circulation mechanism that is created by the film, resulting in a lower temperature difference with respect to the lower plate than without the circulation. When the film velocity reaches its critical value, friction occurs and so the fraction of the total supplied heat that is carried off by circulation diminishes and the temperature differences will start to rise steeper. With respect to the formalism that was developed to describe the distribution of the heat currents this means that R_2 and R_3 become dependent on $\dot{Q}_s$ and $\dot{Q}_u$. The effect of these curved lines results in a less accurate determination of the intersection point where T_u equals T_s. This was especially true when the slopes of both curves near the intersection points were almost equal. Moreover, the intersection point was not always
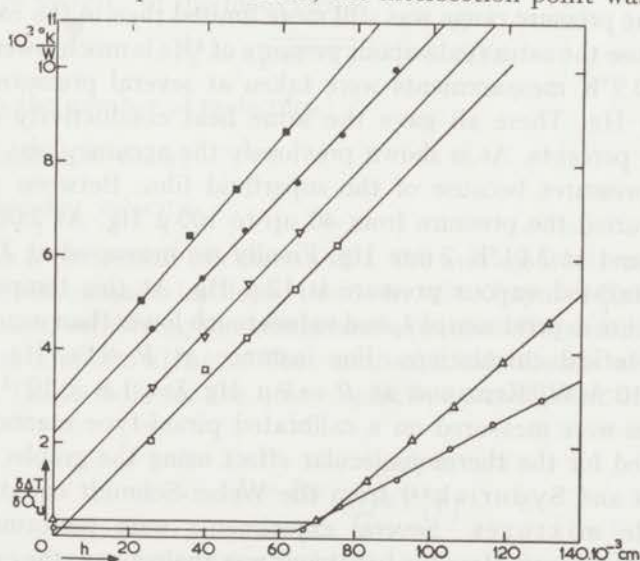
Fig. 12. $\partial(\Delta T)/\partial \dot{Q}_u$ as a function of h in the case of ⁴He, at different temperatures.

■: $T = 0.907°K$	□: $T = 1.547°K$
●: $T = 1.101°K$	△: $T = 2.08°K$
▽: $T = 1.304°K$	○: $T = 3.01°K$

reached, because it became difficult to keep T_l constant at the very high values of $\dot{Q}_s$ that were sometimes necessary to bring the shield ring and the upper plate at the same temperature. In this instance the curves had to be extrapolated. In principle the film has no influence on the method used to derive λ, because R_1 stays independent of the heat currents. This follows since R_1 does not include the resistance of the film adsorbed on u, the direction of the heat current being perpendicular to the upper plate. Thus $T_u - T_l$ will be a linear function of $\dot{Q}_u$, when T_u equals T_s. This is in a-greement with our results.

In fig. 12 $\partial\Delta T/\partial\dot{Q}_u$ is plotted as a function of h for various temperatures. At the low temperatures the vertical scale is shifted to avoid overlapping of the almost parallel and coinciding lines. The values of λ derived from this graph are given in table II.

TABLE II

The heat conductivity coefficient λ for ^{4}He gas	
$T(^\circ K)$	$\lambda(W/^\circ Kcm)$
0.907	3.07×10^{-5}
1.101	3.34
1.304	3.39
1.547	3.48
2.08	4.05
3.01	6.27

For ^{4}He the pressure range was still more limited then in the experiments on ^{3}He, because the saturated vapour pressure of ^{4}He is much lower than that of ^{3}He. At 0.9°K measurements were taken at several pressures between 10 and 30 μ Hg. These all gave the same heat conductivity coefficient within a few percents. As is shown previously the accuracy was smaller at the higher pressures because of the superfluid film. Between 1.1°K and 1.55°K we varied the pressure from 40 up to 100 μ Hg. At 2.08°K it was 0.4 mm Hg and at 3.01°K 2 mm Hg. Finally we measured at $T = 0.8°$K. Here the saturated vapour pressure is 12 μ Hg. At this temperature we found a pressure dependence of λ, and values much lower than were predicted by the theoretical calculations. For instance at $P = 3\mu$ Hg we found $\lambda = 1.45 \times 10^{-5}$ W/$^\circ$Kcm and at $P = 9 \mu$ Hg $\lambda = 1.8 \times 10^{-5}$ W/$^\circ$Kcm. The pressures were measured on a calibrated pirani-type manometer, and were corrected for the thermomolecular effect using the graphs calculated by Roberts and Sydoriak[11]) from the Weber-Schmidt equation.

c) ^{3}He–^{4}He mixtures. Several experiments were performed with a 50% ^{3}He–^{4}He mixture. Here the behaviour was analogous to the experiments with pure ^{3}He. The results are given in table III.

The constant value of $\partial\Delta T/\partial\dot{Q}_u$ at small h is caused by the fact, that a small gap remains between the upper and the lower plate, when the upper

plate is in this lowest position. This is probably caused by a thin rim of the solder, with which the wall is fixed in the lower plate and that lies between the shield ring and the lower plate. The variation of this value of $\partial \Delta T/\partial \dot{Q}_u$ with the temperature is in reality a pressure dependence, for the lower the temperature the lower the pressure has to be. This pressure dependence was checked by doing some measurements with different pressures at the same temperature at $h = 0$.

5. *Theory*. The amount of heat that is transported through a gas is directly related to the transport of kinetic energy by the molecules. If we restrict ourselves to a system with a temperature gradient only in the z-direction, the amount of heat transported through a surface of unit area, which is perpendicular to the temperature gradient and which moves with the average velocity of the molecules is

$$J_z = n\tfrac{1}{2}m\overline{V^2 V_z} = -\lambda \, dT/dz \tag{1}$$

where n is the number of molecules,

m is the molecular mass,

V is the peculiar velocity.

To make a theoretical calculation of λ, the average in (1) must be evaluated. The best method for doing this is by the Chapman-Enskog method, which is based on solving the Boltzmann equation. The details are given in Chapman and Cowling, "The mathematical theory of nonuniform gases" [12]. The formula for the heat conductivity coefficient of a gas of low density is

$$\lambda = \tfrac{5}{2}c_V \frac{5KT}{8\Omega^{(2,2)}(T)} \tag{2}$$

where

$$\Omega^{(2,2)}(T) = \tfrac{1}{2}\sqrt{\pi}\left(\frac{\mu}{2KT}\right)^{7/2} \int_0^\infty \exp\left(-\frac{\mu g^2}{2KT}\right) g^7 Q^{(2)}(g) \, dg \tag{3}$$

17

where μ: the reduced mass of the colliding particles

g: the relative velocity of the colliding particles

K: the Boltzmann constant

$Q^{(2)}(g)$: the total collision cross section

c_V: the specific heat per gram at constant volume.

The total cross section is a weighted average of the differential cross sections, which can be calculated from the two particle problem. Since in our experiments we are concerned with ³He and ⁴He at low temperatures, the two particle problem must be solved using quantum mechanics.

The quantum mechanical differential cross section $\alpha(g, X) \cdot \sin \chi \, d\chi$, where χ is the scattering angle, can be determined by solving Schrödinger's equation $(h^2/2\mu) \, \Delta^2\psi + (\frac{1}{2}\mu g^2 - V) = 0$, where V is the intermolecular field, which is assumed to be angle independent. It appears that the radial wave functions undergo phase shifts $\eta_l(k)$ with respect to the unperturbated problem. These η's are functions of the orbital angular momentum quantum number l and the wave number of relative motion $k = \mu g/h$, and they depend on the potential model that is used. The phase shifts are the only features of a collision that enter in the final quantum mechanical expressions of the transport properties. One finds that

$$\alpha(k, \chi) = \tfrac{1}{4}k^2 \sum_l (2l + 1) \exp\{2i\eta_l(k) - 1\} P_l(\cos \chi).$$

This leads to the expression for the total cross section

$$Q^{(2)}(k) = 2\pi \int_0^\pi (1 - \cos^2\chi) \, \alpha(k, \chi) \sin \chi \, d\chi =$$

$$= (2\pi/k^2) \sum_l (l + 1) \cdot (l + 2)(l + \tfrac{3}{2}) \sin^2\{\eta_{l+2}(k) - \eta_l(k)\}.$$

In order to calculate $Q^{(2)}(k)$ only the phase shifts must be calculated for different values of l.

For indistinguishable particles, which obey Bose Einstein statistics and have zero spin, l is even. This is designated by $Q^0_{\text{B.E.}}$. For indistinguishable particles, which obey Fermi Dirac statistics and have zero spin, l is odd. This is similarly designated by $Q^0_{\text{F.D.}}$. And l is both even and odd for distinguishable particles.

If the spin $S \neq 0$ the matter is more complicated. For atoms consisting of an even number of particles the total wave function must be symmetrical, according to the Ehrenfest-Oppenheimer rule[13]. In our problem we have to deal only with the radial wave function and the spin wave function of the total wave function. Therefore the product of the spin- and radial wave functions must be symmetrical. For a system of two particles with a nuclear spin, every state is $(2s + 1)^2$ — fold degenerate. Of these different spin

18

wave functions $(s + 1)(2s + 1)$ are symmetrical, and $s(2s + 1)$ are anti-symmetrical. To get a symmetrical total wave function the former must be multiplied by a symmetrical radial wave function and the latter with an antisymmetrical one.

Therefore the states with a symmetrical radial wave function appear with a weight $(s + 1)/(2s + 1)$ and those with an antisymmetrical one with the weight $s/(2s + 1)$. This gives for the total cross-section for B.E. particles with spin s:

$$Q^s_{\text{B.E.}} = \frac{s + 1}{2s + 1} \, Q^0_{\text{B.E.}} + \frac{s}{s + 1} \, Q^0_{\text{F.D.}}. \tag{4}$$

It is clear that for atoms consisting of an odd number of particles, *i.e.* those with an antisymmetrical total wave function, the weighting factors have changed place. This gives the expression

$$Q^s_{\text{F.D.}} = \frac{s}{2s + 1} \, Q^0_{\text{B.E.}} + \frac{s + 1}{2s + 1} \, Q^0_{\text{F.D.}}. \tag{5}$$

Since ^{4}He has an even number of particles and zero spin, we get from formula (4), $Q_{^4\text{He}} = Q^s_{\text{B.E.}} = Q^0_{\text{B.E.}}$. Thus in this case the phase shifts $\eta_l(k)$ have to be calculated only for even l. As ^{3}He has an odd number of particles and spin $s = \frac{1}{2}$ formule (5) gives $Q_{^3\text{He}} = Q^{\frac{1}{2}}_{\text{F.D.}} = \frac{1}{4}Q^0_{\text{B.E.}} + \frac{3}{4}Q^0_{\text{F.D.}}$. Now the phase shifts $\eta_l(k)$ have to be calculated for even as well as odd values of l. This symmetrization of the wave functions causes an important difference between the transport properties of ^{3}He and ^{4}He.

Moreover a further difference between these gases is the fact that ^{4}He has a real or virtual stationary state at very small relative wave numbers, which is not the case with ^{3}He. This means that at $l = 0$ and when k is very small $\eta_0(k)$ is proportional to $\frac{1}{2}\pi - k\sigma$ for ^{4}He, where σ is the diameter of the atom. This leads to $Q^{(2)} \sim k^{-2}$. If one introduces this in the formulae (2) and (3), it is easily seen that $\lambda \sim T^{\frac{1}{2}}$ at $T = 0°$K.

In the case of ^{3}He $\eta_0(k)$ is proportional to $K\sigma$. This leads to a constant value of $Q^{(2)}$. If this is introduced in (2) and (3) it follows that $\lambda \sim T^{\frac{1}{2}}$ at $T = 0°$K.

Calculations based on this theory have been performed by several authors for several different intermolecular potentials. Since the interaction potential is not known with enough precision, a curve is generally assumed of the type indicated by purely theoretical considerations but with constants that can be determined experimentally. For the repulsive part either an exponential term, or a twelfthpower term is used. The attractive part is represented by a sixth power term, which is related to virtual dipole-dipole interation, and an eighth power term related to virtual dipole-quadrupole interaction. The constants that are to be determined are the minimum value of the potential (ε), and the distance between the molecules when the potential is zero (σ) or where the potential has its minimum value, (r_m).

19

The first calculations of the transportproperties of ^{4}He were done by Buckingham, Hamilton and Massey, for several potentials and three values of the constants that were not well known at that time. Several years later De Boer calculated the transport properties of ^{4}He using a Lennard-Jones type potential with 6–12 power laws:

$$\varphi(r) = 4\varepsilon \left[\left(\frac{\sigma}{r} \right)^{12} - \left(\frac{\sigma}{r} \right)^{6} \right],$$

with $\varepsilon = 14.11 \times 10^{-16}$ erg and $\sigma = 2.556$ Å. These constants are obtained from a best fit of the second virial coefficient for ^{4}He gas at high temperatures. De Boer calculated as well the first as well as the second approximation.

In 1951 Cohen and De Boer calculated the transport properties of ^{3}He with the same potential, and in 1954 Cohen, Offerhaus and De Boer did it for ^{3}He–^{4}He mixtures. In both cases only the first approximation was used. Buckingham and Scriven used an exp − 6–8 potential for their calculations

$$\varphi(r) = \varepsilon \left[f_1 \exp\left(-\frac{\alpha r}{r_{\rm m}} \right) - f_2 \left(\frac{r_{\rm m}}{r} \right)^{6} - \beta f_2 \left(\frac{r_{\rm m}}{r} \right)^{8} \right].$$

$\varepsilon = 14.04 \times 10^{-16}$ erg and $r_{\rm m} = 2.943$ Å. $\alpha = 13.6$ and $\beta = 0.2$. The constants f_1 and f_2 are functions of α and β. They are also derived from the best fit with the second virial coefficient data at high temperatures. By applying Keller's corrections, we calculated the second approximation for this intermolecular potential.

Keller calculated the viscosity coefficient of ^{3}He and ^{4}He using a Lennard-Jones potential, as well in the first as well as in the second approximation. He used an electronic computer, to be able to compute more phases. This enables a more accurate calculation of λ. The theoretical curves are drawn in fig. 13 where our experimental values are also shown. In the ^{4}He case, there is a good agreement between Keller's and De Boer's values, but in the ^{3}He case a rather large difference exists, which is already present in the phases. This is probably caused by the greater accuracy Keller could attain.

At the lowest temperatures there is no difference between the results obtained with a Lennard-Jones potential and those with an exp − 6–8 potential. At higher temperatures the former gives in the ^{3}He case a somewhat higher value, while in the ^{4}He case the difference stays small. It is clear from the Schrödinger equation, that the influence of the potential for ^{3}He is larger than for ^{4}He because of the difference in mass between both isotopes.

In fig. 13 are also shown the values of the heat conductivity coefficient

that can be obtained from the experimental viscosity coefficients measured by Becker, Misenta and Schmeissner.[10]
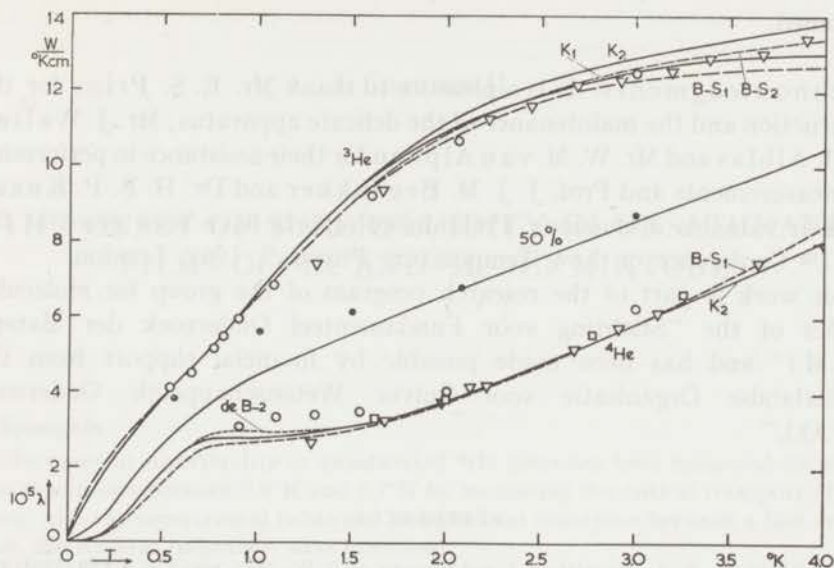
Fig. 13. The heat conductivity coefficient λ as a function of the temperature.

O: ^{3}He and ^{4}He measured by the authors.

□: ^{4}He measured by Ubbink[7]).

▽: ^{3}He and ^{4}He calculated from the viscosity data of Becker, Misenta and Schneisner[10]

——— K_1: calculated by Keller, first approximation[6])

——— K_2: calculated by Keller, second approximation

– – – B–S$_1$: calculated by Buckingham and Scriven, first approximation[5]).

– – – B–S$_2$: second approximation of the Buckingham-Scriven method, calculated by the authors, by applying the correction that K_2 makes on K_1.

------ Second approximation calculated by De Boer[2]).

●: 50% ^{3}He–^{4}He mixtures measured by the authors.

——— 50%: calculated by Cohen, Offerhaus and De Boer[4]).

Comparing our results with the theoretical curves, we observe the following facts. Very good agreement exists for ^{3}He below 1°K; above 1°K our values are lower than the theoretical ones, but we agree with Becker's experiments. For ^{4}He our values are somewhat higher than the theoretical predictions. There is satisfactory agreement with the experiments of Ubbink. Observing our results with a 50% ^{3}He–^{4}He mixture we see that above 2°K there is good agreement with the theoretical values of Cohen, Offerhaus and De Boer. Below 2°K, however, a deviation occurs, probably caused by the fact, that the concentration of ^{3}He in the gaseous phase is larger than in the layer that is absorbed at the wall – this is analogous to the concentration difference between vapour and liquid for a mixture of ^{3}He

and ^{4}He. This difference from the theoretical curve increases at lower temperatures, so at $T = 0.53°$K the heat conductivity coefficient we measured is almost that of pure ^{3}He, The experiments with ^{3}He–^{4}He mixtures are continued.

Acknowledgments. It is a pleasure to thank Mr. E. S. Prins for the ocnstruction and the maintenance of the delicate apparatus; Mr. J. Walter, Mr. H. Alblas and Mr. W. M. van Alphen for their assistance in performing the measurements and Prof. J. J. M. Beenakker and Dr. H. F. P. Knaap for their valuable discussions. Preliminary reports have been given at the "VIIIth Conference on Low Temperature Physics", 1962, London.

REFERENCES

1) Buckingham, R. A., Hamilton, J. and Massey, H. S. W., Proc. roy. Soc. A 179 (1941) 103.
2) De Boer, J., Physica 10 (1943) 348. Progress in Low. Temp. Phys., Ed. C. J. Gorter (North Holland Publ. Co. Amsterdam, 1955) p. 381.
3) De Boer, J. and Cohen, E. G. D., Physica 17 (1951) 993.
4) Cohen, E. G. D., Offerhaus, M. J. and De Boer, J., Physica 20 (1954) 501.
5) Buckingham, R. A. and Scriven, R. A., Proc. phys. Soc. London B 65 (1952) 376.
6) Keller, W. E., Phys. Rev. 105 (1957) 41.
7) Ubbink, J. B., Thesis, Leiden (1945).
   Ubbink, J. B. and De Haas, W. J., Commun. Kamerlingh Onnes Lab., Leiden No. 266d; Physica 10 (1943) 465.
   Ubbink, J. B., Commun. Leiden, Suppl. No. 96b; Physica 13 (1947) 659.
8) Challis, L. A., Thesis, Oxford (1957).
9) Van Itterbeek, A., Schapink, F. W., Van den Berg, G. J. and Van Beek, H. J. M., Commun. Leiden No. 294b; Physica 19 (1953) 1158.
10) Becker, E. W., Misenta, R. and Schmeissner, F., Z. für Physik 137 (1954) 126.
11) Roberts, T. R. and Sydoriak, S. G., Private Communication, University of California, Los Alamos Laboratories, New Mexico, U.S.A.
12) Chapman, S. and Cowling, T. G., The mathematical theory of non uniform gases (Cambridge University Press, 1952).
13) Ehrenfest, P. and Oppenheimer, J. R., Phys. Rev. 37 (1931) 333.
14) Van Itterbeek, A. and Keesom, W. H., Commun. Leiden No. 252a; Physica 5 (1938) 257.

THE ONSET OF SUPERFLUIDITY IN UNSATURATED FILMS OF ^{4}He AND ^{3}He–^{4}He MIXTURES

Synopsis

The onset of superfluidity in unsaturated ^{4}He films has been measured for several film thicknesses between 0.8°K and 1.7°K by measuring the critical transport of these films. Also the supercritical behaviour and the heat resistance between a film and the wall, the Kapitza resistance, were examined.

For mixtures, which had at room temperature a concentration of respectively 50%, 80% and 90% ^{3}He, the onset of superfluidity was measured between 1.3°K and 1.8°K. In this region also adsorption isotherms of these mixtures were measured.

1. *Introduction.* A surface, that is in contact with liquid He II is covered by a multilayer film, which has superfluid properties. The "Kamerlingh Onnes effect" (1922)[1] (the levelling of the surfaces of helium in two open vessels, having a common wall) was the first indication for its existence, although this conclusion was not yet drawn then, but much later in 1936, when Rollin[2] postulated the existence of the film to explain the anomalous heatflow in all kinds of experiments. Its properties were examined carefully by Daunt and Mendelssohn[3] and later by many others[4]. The most important properties are that the rate of flow of a film depends only on the smallest width of the path and on the temperature, but not on the pressure head. The experiments led to the concept of a critical velocity, v_c, of the film, which determines a critical mass transfer. The fact, however, that the critical transfer rates measured by different authors disagree is caused by the important influence that structure and contamination of the surface on which it is adsorbed have on the film.

In 1950 Long and Meyer[5] discovered, that an unsaturated film often demonstrates superfluidity too. From their measurements on mass transfer, and from heat transport measurements by Bowers, Brewer and Mendelssohn[6], Long and Meyer[7] and Brewer and Mendelssohn[8] can be concluded that above a certain value of the ratio P/P^0, where P is the

pressure and P^0 the saturated vapour pressure, superfluidity appears. These critical values of P/P^0, hereafter indicated as $(P/P^0)_c$ have been measured by the above mentioned authors between 1.3°K and the λ-point of the bulk liquid and were found to be temperature dependent. At the same time the critical transfer through such a multilayer superfluid film was measured by them.

Several authors[9]) have tried to explain the lowering of the λ-point and with it the possibility of superfluidity in unsaturated films, by calculating the condensation temperatures of a Bose-Einstein system in samples of finite dimensions $L \times L \times D$, with $D \ll L$. Also Ginzburg and Pitaevskii[10]) developed a phenomenological model analogous to the Ginzburg-Landau theory on superconductivity. In both ways a qualitative description is obtained.

In heat conductivity measurements of gaseous ^{4}He the unsaturated film can introduce a disturbing extra heat transfer as was already mentioned in our previous article on heat conductivity[11]). As the apparatus used then was provided with a ^{3}He cryostat, we were able to measure $(P/P^0)_c$ values in it between 0.9°K and 1.3°K; a temperature region that was not studied before. In this apparatus we also measured the onset of superfluidity in ^{3}He–^{4}He mixtures for various concentrations, of which the results are presented in reduced phase diagrams. As the apparatus was not designed for this purpose and especially the geometry was not ideal a second apparatus was built consisting of a glass cylinder closed at the top and provided with a heater, whereas the lower end was in thermal contact with a ^{3}He cryostat. In this way the apparatus, that is very similar to those used by the previously mentioned investigators, was suitable to measure not only the onset of superfluidity, but also the critical transfer rates for various values of P/P^0. As a third result we could derive the heat resistance between the film and the solid wall - the Kapitza resistance. It is still impossible to give our results as a function of the thickness of the film, as is desirable in order to make a comparison with theoretical calculations, due to the fact that good adsorption isotherms in the temperature region below 1.3°K are available neither for ^{4}He nor for ^{3}He–^{4}He mixtures. In the supercritical region we examined the dependence of the transport on the gradient in the chemical potential.

2. *The method.* First we shall describe the heat transport mechanism in a vessel of which the walls are covered with an adsorbed helium film.

Let there be a cylinder c as in fig. 1 with a smooth inner surface and such dimensions that the heat resistance, when filled only with gas, is high. The bottom b is kept at a constant temperature, the top t can be heated by the heater h. When no film is present on the wall, neither superfluid nor normal fluid, the heat supplied to t will be carried off by normal heat
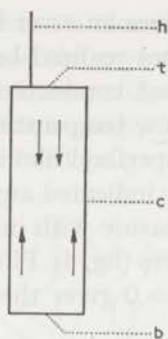
Fig. 1. Scheme of the film flow apparatus; arrows indicate the circulation. Explanation of the symbols is in the text.

conduction through the gas. When an immobile film is adsorbed, this film will partly evaporate at t, but the loss cannot be replenished, so that a steady state equivalent to the first is obtained. However, when a superfluid mobile film is present the loss caused by evaporation will still be replenished, so that a mass current takes place in the gaseous state from the top to the bottom and through the film back to the top. Due to this convection, the direction of which is indicated by arrows, only a small temperature difference appears between t and b. In equilibrium the amount of heat supplied to t is:

$$Q = (L + TS)\,\dot{m} = TS_g\dot{m}$$

where L is the latent heat, TS the thermomechanical term, S_g the entropy of the gas and $\dot{m}$ the amount of mass that is transported per second. As the film is bound to a maximum velocity v_c, only a limited amount can be transported $\dot{m}_c = 2\pi r v_c d\rho_s$ where r is the radius of the tube, d the thickness of the film and ρ_s the density of the superfluid part of the film. So it is easy to see, that when the amount of heat Q becomes higher than a certain critical value Q_c, more helium is evaporated than can be supplied by the film. So the convection comes to an end in the upper part of the cell and the temperature difference suddenly starts to rise. When the convection has died out, here the temperature difference is determined by the normal heat conduction.

From this mechanism one can obtain two methods to measure $(P/P^0)_c$. The first consists of measuring the temperature difference ΔT between top and bottom, at a constant small heat input as a function of the pressure. At equilibrium pressures below $(P/P^0)_c$ ΔT is determined by the heat transported by the gas and by the accommodation coefficient. As long as the heat conductivity coefficient of the gas does not depend on the pressure, ΔT remains constant with increasing pressure, till the film on the wall becomes superfluid and ΔT suddenly decreases, because now the convection

25

sets in. This method always gives an error because $(P/P^0)_c$ is defined at a zero heat current and this is not realized here. Moreover, when mean free path effects make that the heat conductivity becomes depending on the pressure which is the case at low temperatures, ΔT decreases already with increasing pressure, when no superfluid film is present. Thus the point where superflow sets in is not sharply indicated any more.

The second method is to measure with increasing heat input the critical heat current for various pressures (fig. 4). Plotting then these $\dot{Q}$ as a function of P/P^0 to extrapolate to $\dot{Q}_c = 0$ gives the value of P/P^0 where the film becomes superfluid (fig. 5).
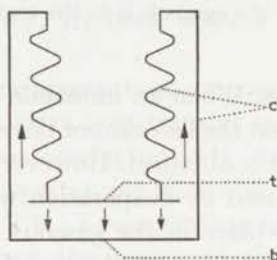
Fig. 2. Scheme of the first apparatus, the same symbols as in figure 1.

The first method was used to determine the onset of superfluidity in films consisting of ^{3}He–^{4}He mixtures and originally also for ^{4}He. As the apparatus (schematically shown in fig. 2) was constructed in such a way that the thermal resistance of the gas was low, ΔT could not become very large. Moreover, since its walls, consisting of bellows, were not smooth and had varying diameters, it was not suitable for correct measurements of $\dot{Q}_c$. Therefore a new apparatus was built to use method two. The construction is given in section 3.

3. *The apparatus.* As the first apparatus is fully described in chapter I[11]), we will discuss here only the second one. A drawing of it is given in fig. 3. It consists of a glass tube a with inner diameter of 4.7 mm and length 5 cm. It is closed at the top with the copper block k. To this block are soldered the carbon thermometer of the de Vroomen-type e and the heater f. The glass tube is at its lower end connected to the copper block l, in which are drilled the holes b and c; b is a part of the adsorption space. This space is filled through the stainless steel tube d. Originally it was a capillary with diameter 180 μ. Later it was replaced by a tube with inner diameter 2 mm, to avoid a disturbing pressure drop over it as will be discussed in the next subsection. Space c is a ^{3}He-cryostat, that is pumped off through the stainless steel tube g; n and m are respectively a thermometer and a heater. The part h is the top plate of the vacuum jacket that surrounds the

apparatus. Here d and g pass into stainless steel tubes with $\frac{1}{2}$ inch diameter. The adsorption space is outside the cryostat connected to a manometer system consisting of an oil manometer filled with Octoil-S, (the levels are read with a cathetometer), a Pirani gauge, (the scale was calibrated against the oil manometer), and a Mac Leod gauge. All pressures were corrected for
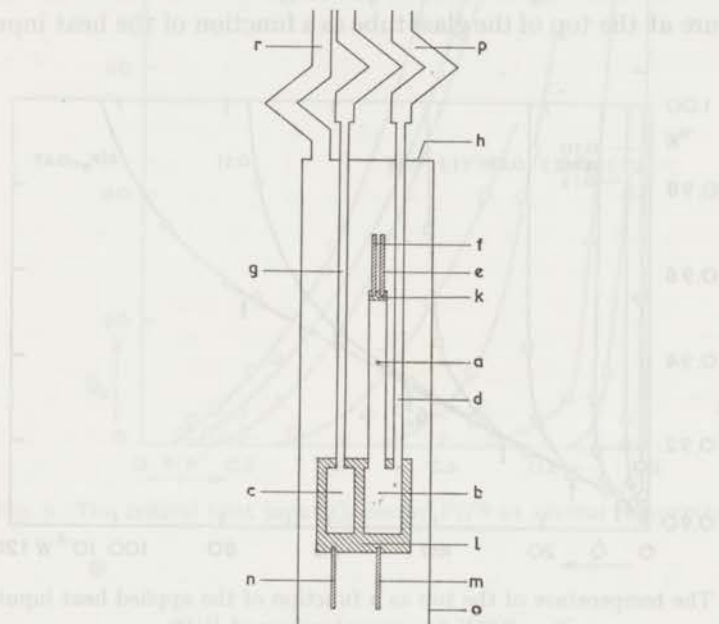
Fig. 3. Second apparatus. Explanation of the symbols is in the text.

the thermo-molecular pressure difference according to graphs calculated by Roberts and Sydoriak[12]) from the Weber-Schmidt equation[13]).

In our first measurement a 180 μ capillary connected the adsorption space to the $\frac{1}{2}$ inch filling line, to diminish the heat leak. With this construction we found that below 1°K the critical heat currents were smaller than at higher temperatures at the same value of P/P^0. This could only be understood by assuming that the value of P we measured was too high. This is caused without doubt by the fact that a temperature gradient exists along the capillary, since the outer bath is at 1.3°K and the adsorption space is at a lower temperature. As a consequence it forces the film that is adsorbed in the capillary to move to the higher temperature .There it evaporates and gas has to flow back and to recondense in b. When the gas has a low pressure a relative large pressure difference is necessary to transport the gas back, especially when the mean free path becomes of the order of the diameter of the the capillary. So at the top of the capillary the pressure, which is the pressure we measure, is higher than in the adsorption space. Therefore we replaced

27

it by a tube with 2 mm diameter. We indeed measured the same critical heat currents at much lower pressures already. Finally this wide tube had the disadvantage that we were not able to measure at high values of P/P^0 at the lowest temperatures due to the heat leak which was introduced.

4. *The results.* In fig. 4 an example is given of the behaviour of the temperature at the top of the glass tube as a function of the heat input $\dot{Q}$ for
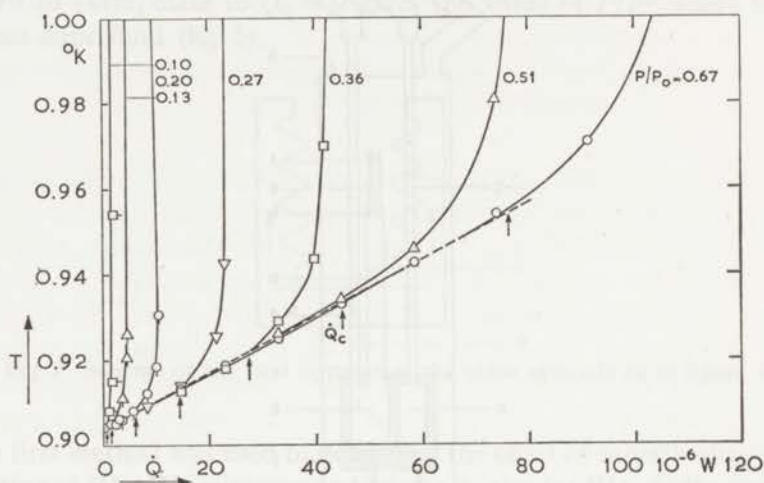
Fig. 4. The temperature of the top as a function of the applied heat input $\dot{Q}$ at $T = 0.9°$K for several values of P/P^0.
arrows indicate the critical heat input $\dot{Q}_c$
— — — the Kapitza temperature drop between the wall and the adsorbed helium.

TABLE I

$T = 0.812°$K		$T = 0.904°$K		$T = 1.000°$K		$T = 1.167°$K	
P/P^0	$\dot{Q}_c$	P/P^0	$\dot{Q}_c$	P/P^0	$\dot{Q}_c$	P/P^0	$\dot{Q}_c$
0.088	2.5×10^{-6} W	0.105	0.5×10^{-6} W	0.162	0.5×10^{-6} W	0.30	2×10^{-6} W
0.10	4.0	0.131	2	0.20	2	0.45	5
0.15	5.9	0.197	5	0.275	7	0.57	23
0.22	12	0.268	14	0.39	20	0.68	40
0.38	32	0.36	18	0.525	40		
0.54	68	0.509	44	0.74	95		
		0.665	78				

$T = 1.29°$K		$T = 1.51°$K		$T = 1.72°$K	
P/P^0	$\dot{Q}_c$	P/P^0	$\dot{Q}_c$	P/P^0	$\dot{Q}_c$
0.60	6×10^{-6} W	0.70	1×10^{-6} W	0.92	12×10^{-6} W
0.655	12	0.795	4	0.96	40
0.75	40	0.85	8		
0.775	47	0.89	32		
		0.96	96		

Fig. 5. The critical heat input $\dot{Q}_c$ *versus* P/P^0 at several temperatures.
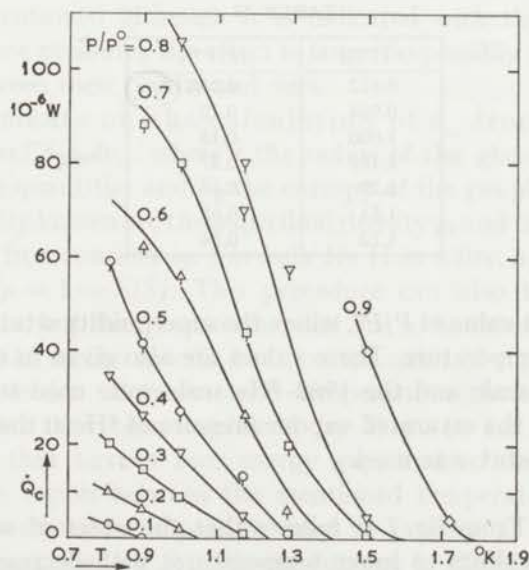
Fig. 6. The critical heat input $\dot{Q}_c$ *versus* T at several constant values of P/P^0.

different values of P/P^0. One sees that all curves have a coinciding linear part up to a certain value of $\dot{Q}$, where the temperature starts rising more rapidly. This value of $\dot{Q}$ is called the critical heat current $\dot{Q}_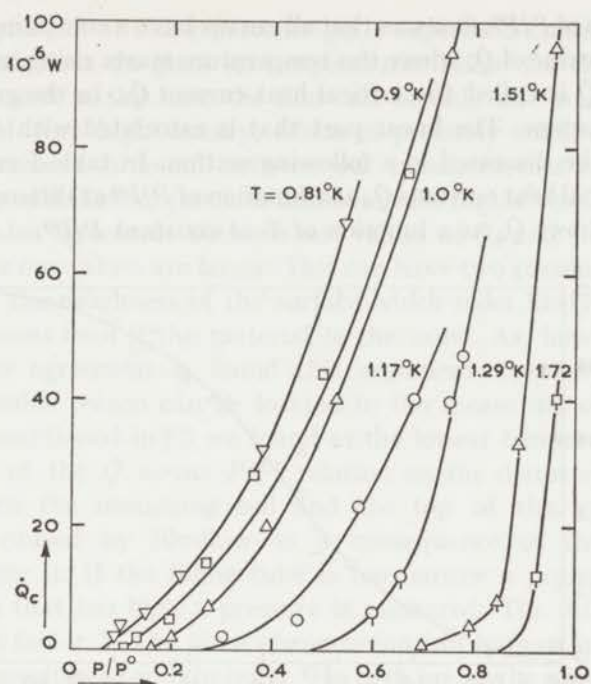c$. In the graph it is indicated by an arrow. The linear part that is associated with the Kapitza resistance will be discussed in a following section. In table I and fig. 5 are shown the critical heat currents $\dot{Q}_c$ as a function of P/P^0 at different temperatures. Fig. 6 shows $\dot{Q}_c$ as a function of T at constant P/P^0.
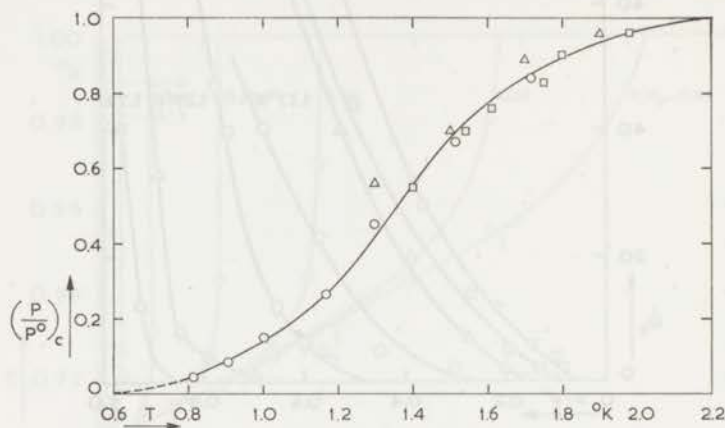
Fig. 7. The onset of superfluidity expressed in values of P/P^0, $(P/P^0)_c$, versus T
        △   Long and Meyer [7])
        □   Brewer and Mendelssohn [8])
        ○   this article

TABLE II

$T(^\circ K)$	$(P/P^0)_c$
0.812	0.055
0.904	0.10
1.000	0.15
1.167	0.27
1.29	0.45
1.51	0.65
1.72	0.84

Fig. 7 gives that value of P/P^0, where the superfluidity sets in, $(P/P^0)_c$, as a function of the temperature. These values are also given in table II.

The 1958–^{4}He scale and the 1962–^{3}He scale were used to calculate the temperatures and the saturated vapour pressure of ^{4}He at the temperatures, where a ^{3}He-cryostat was used.

5. *Discussion*. From fig. 7 it follows that the onset of superfluidity in unsaturated films shifts to lower temperatures with decreasing thickness. It also shows that already very thin films, with a thickness corresponding

to a value of P/P^0 of a few percents get a superfluid character. Although no adsorption data on glass at temperatures below 1.3°K are available, we suggest, that in this case the film can be only one layer thick, if the first layer of very high density, which is probably solid, is disregarded.

Good agreement is found between our measurements of the onset of superfluidity and those of previous authors in the higher temperature region.

There is also agreement between our values of $\dot{Q}_c$ and theirs, except at 1.3°K, where our values are larger. This can have two reasons. The first can be found in the roughness of the surface which most likely is different in each experiment even if the material is the same. As, however, at higher temperatures agreement is found this argument has very little value. Another possible reason can be located in the measuring of the pressure. As already mentioned in § 3 we found at the lowest temperatures a strong dependence of the $\dot{Q}$ *versus* P/P^0 relation on the diameter of the filling tube between the measuring cell and the top of the vacuum jacket, which was caused by filmflow as a consequence of the temperature gradient along it. If the filling tube is too narrow a pressure gradient is produced so that too high a pressure is measured. The difference can be more than a factor 2. The same phenomenon can happen in an apparatus in which measuring cell and the outer ^{4}He bath are at the same temperature, but now if the filling tube to the top of the cryostat has too small a diameter. In the part of this tube above the liquid helium level a film flow also will occur as a consequence of the temperature gradient there, which will lead to a higher pressure in the manometers. In the publications of Long and Meyer[7]) and Brewer and Mendelssohn[8]) the diameter of their filling tube is not mentioned although it is indicated with the word capillary. Especially at low pressures the effect is large. So possibly it can explain the difference between their results and ours.

Some comments on the calculation of v_{s_c} from $\dot{Q}_c$. As already stated $\dot{Q}_c = 2\pi r T S_g \rho_s dv_{s_c}$ where r the radius of the glass tube, T and $\dot{Q}_c$ are well known quantities and S_g the entropy of the gas phase easily can be calculated. Badly known are the superfluid density ρ_s and the thickness of the film. Let us at first consider ρ_s. For bulk He II in a first approximation one may write $\rho_s/\rho = 1 - S/S_\lambda$. This procedure can also be applied to an unsaturated film, but the question is, what has to be taken as the λ-temperature; the "peak" in the specific heat, or the onset of superfluidity for the thickness in question. Between both temperatures there is a remarkable difference, which has been explained by Brewer *e.a.*[29]) by means of surface waves that have a zero energy gap, and so thus a zero critical velocity in the region between the mentioned temperatures. This means that ρ_s is zero there. So a possible way to express ρ_s is by means of $\rho_s/\rho = 1 - S/S_{onset}$, where S_{onset} is the entropy of the film at the temperature where the superfluidity sets in.

As T_{onset} is lower than T_λ, S_{onset} will be lower than S_λ – the subscript λ indicates here the specific heat peak –, which leads to a value of v_{s_o}, that is about a factor of two larger. If one treats the experimental data in this way values of v_{s_o} can be derived which are proportional to the thickness and are of the order of 100 cm s^{-1} to 300 cm s^{-1} for $T < 1.2°$K. For the thickness of the film we used values derived from Brewer *e.a.* [29]).

Long and Meyer [7]) applied a rather simplified model. They plotted $\dot{Q}_c$ versus the number of layers ν and said $\partial \dot{Q}_c/\partial \nu$ is the differential amount of heat carried per added layer. That means that there are some immobile layers with upon them purely superfluid layers. As $\dot{Q}_c$ is almost a linear function of ν at least above $T = 1.5°$K the velocity of each added layer remains the same in this case. Long and Meyer claim a variation of maximal 30%, but observing their graphs, we get the impression that for higher thicknesses the slope changes with more than a factor two. Applying this procedure on our measurements gives velocities of the same order of magnitude, as the other method. The accuracy, however, is very small.

Discussion of the linear part of the ΔT versus $\dot{Q}$ curve. As stated already in § 4 a feature of fig. 4 needs attention, because for all values of P/P^0 the temperature of the top of the glass tube rises with the same slope with increasing $\dot{Q}$. As inside the apparatus the temperature can be expected to be constant because of the superfuidity of the film, this linear temperature rise must be found in the heat resistance between the wall and the film. In experiments with bulk helium this resistance between helium and wall is known as the Kapitza resistance. Although many experiments have been
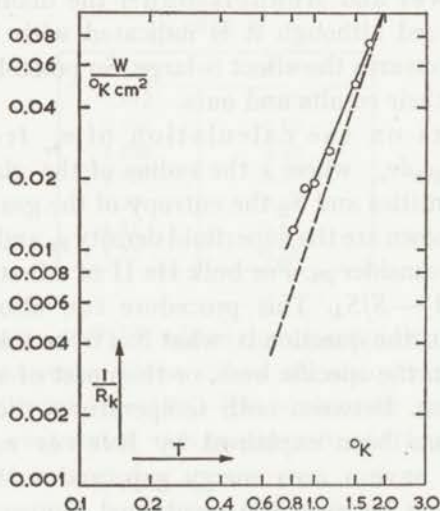

Fig. 8. A double logarithmic graph showing the inverse of the Kapitza resistance
versus T.
  o   experimental values with exponent 2.4
– – –   theoretical values of Khalatnikov with exponent 3.

done on this subject[14]) up to the present time a good explanation of this phenomenon has not yet been given. From our results can be concluded, that also for the thinnest films the effect occurs, so that most probably this temperature jump must be located between the wall and the first layer. In fig. 8 we have drawn the values of the inverse of $\frac{1}{2} O \, \partial T/\partial \dot{Q} = R_k$ – see also table III – as a function of the temperature – both on a logarithmic scale.

TABLE III

$T(°K)$	$1/R_K$ W/°K cm²
0.812	0.012
0.904	0.018
1.000	0.019
1.167	0.026
1.29	0.036
1.51	0.052
1.72	0.074

Here O is the surface of the copper block that closes the glass tube at the top. The factor two arises from the fact, that the heat current twice passes a transition plane between solid and film, once at the top and once at the bottom of the cell. From the graph follows a $T^{2.4}$ dependence on the temperature. This is what is generally found for copper with a normal rough surface. The dotted line is the theoretical prediction of Khalatnikov[15]), which shows a bad agreement with our points. The absolute values of the Kapitza-resistance measured by us are of the same order as those measured by Fairbank and Wilks[16]), but higher than those found by Kuang Wey Yen[17]).

Discussion of the nonlinear part of the ΔT versus $\dot{Q}$ curve. In section 2 we stated that as soon as the critical transport is reached a sudden temperature rise would occur. From our measurements we find, however, a rather gradual one. The temperature difference ΔT along the film – $i.e.$ the temperature difference between upper and lower plate minus the temperature jump caused by the Kapitza resistance – rises exponentially with the extra heat input $\dot{Q} - \dot{Q}_c$. We have tried to find some systematics in this behaviour. The flow of superfluid helium is often found to be governed by the gradient in the chemical potential μ. As $d\mu = -S \, dT + V \, dP$ the total difference in chemical potential along the film is

$$\Delta \mu = -\int_T^{T+\Delta T} S \, dT + \int_P^{P+\Delta P} V \, dP.$$

The dimensions of the glass tube on the wall of which the film flows are such that the pressure gradient can be neglected. So only $\int_T^{T+\Delta T} S \, dT$ has to be calculated. As values for S we used the data calculated by Long and Meyer[18]) by integrating the specific heat data of Frederikse[19]), who measured the

33

specific heat of unsaturated films adsorbed on jewellers rouge. We calculated $\Delta\mu$ as a function of $\dot{Q}/TS_g$, where S_g is the entropy of the gas phase. As already mentioned $\dot{Q} = (L + TS_1) 2\pi r \, d\rho_s v_s$ where $L = T(S_g - S_1)$. So

$$\dot{Q} = TS_g 2\pi \, r d\rho_s v_s \text{ and } \dot{Q}/TS = 2\pi \, r d\rho_s v_s.$$

S_g is calculated following

$$S_g = R \ln \{(KT)^{\frac{5}{2}} (m/2\pi\hbar)]^{\frac{3}{2}} P\}$$

where K is Boltzmann's constant, P the pressure of the gas, $\hbar$ Planck's constant and m the mass of a helium atom.

We found that

$$\Delta\mu = A (\rho_s v_s d)^n.$$

It appears that in most cases $n = 11$. The factor A is proportional to the critical transport rate.

A similar behaviour as described above can be found in what some authors call the region of subcritical flow of saturated helium films, but that we call already supercritical flow. Atkins[24]) gives in a diagram of the frictional force *versus* the velocity an example of "mixed flow", consisting of a frictionless part up to a certain critical velocity, and a pressure dependent part, which can raise the velocity above the critical one.

Chandrasekhar and Mendelssohn[25]) examined the subcritical flow in the helium II film by means of thermomechanical film transfer. They found flow rates that started as a linear function of the heat input, which means pure superflow, but after this a curved section followed, in which the dependence of the flow rate on the heat input became slower, till the flow rate becomes constant. The authors suppose that the geometry of the apparatus, which causes a radial flow of the film, is the reason of the curved part.

Experiments on film flow at low pressure heads have also been published by Seki[26]). He measured the film flow from a surrounding bath into a beaker as a function of the amount of heat supplied to a heater submerged in the helium inside the beaker. The results show at the lowest effective pressures – *i.e.* thermomechanical pressure minus height difference – pure superflow, till the flow rate reaches a critical value, above which the flow rate is a linear function of the effective pressure head. At still higher effective pressures the flow rate rises ever slower, till it becomes independent of the driving force. It is difficult to make comparisons with our results because it is impossible to calculate the gradient in the chemical potential from their data as the temperature differences are not published. But the character of the results seems to be the same.

In channels with 0.4 cm till 50 μ diameter Van Alphen *e.a.*[27]) found a quadratic dependence of the gradient in the chemical potential on the velocity

of the superfluid. In slits with width of the order of a micron, Wansink[28]) found that the pressure difference along the slit could be described with the 3.45 power of the superfluid transport. This suggests that the exponent is a function of the thickness and gets larger when the thickness decreases.

6. *Theory.* Two methods have been applied to calculate the shift of the λ-point in helium films with decreasing thickness. As ^{4}He follows Bose-Einstein statistics, at a certain temperature the Bose-Einstein condensation will take place. This means that at that temperature T_c a finite fraction of all particles will be in the same state. In the case of helium-4 this is the ground state. London pointed out that the λ-phenomenon in liquid ^{4}He is such a condensation. In principle only in infinite systems a sharp transition can be defined. When the same procedure as used to calculate T_c in infinite systems is applied on finite systems as ^{4}He-films a sharp transition cannot be expected, as at temperatures above T_c the ground state is already partially filled. As Goble and Trainor[30]) point out it is better to speak of a transition region, where the thermodynamic quantities change rapidly. This region can however be characterised by a transition temperature. For thin films, that means for a geometry $L \times L \times D$, where $D \ll L$, these temperatures have been calculated in the case of an ideal Bose-Einstein gas[9]). As helium does not behave as an ideal gas, good agreement with experiment cannot be expected. A more realistic way is to calculate it for a non-ideal gas. This was done by Singh and Pathria. They found a reasonable agreement with the Long and Meyer data for temperatures far enough from the λ-point of bulk ^{4}He. *i.e.* for not to thick films. They pointed out that although in the ideal gas case the boundary conditions are very important, in the non-ideal gas case they became rather unimportant, but now the contributions arising from the presence of surface waves on the liquid surface had to be taken into account.

The properties of helium near the λ-point can also be described with the approach as is applied in the phenomenological theory of phase transitions of the second order, although it is not quite sure that the λ-phenomenon is such a transition. In this theory the thermodynamic potential is expanded in a series of powers of an order parameter ψ. This was done by Ginzburg and Pitaevskii[10]) in a way analogous to the treatment of superconductivity by Landau and Ginzburg. The order parameter ψ is the true wave function of superfluid helium: $\psi(x, y, z) = \eta \, e^{i\varphi}$. The superfluid density and velocity can be expressed in ψ and φ: $\rho_s = m \, |\psi|^2$ and $v_s = (\hbar/m) \, \nabla\varphi$ where m is the mass of the helium atom. Above the transition temperarure ψ is zero and at the other side non zero. In the latter case the value of ψ is determined by requiring the thermodynamic potential to be minimal with respect to ψ. Together with the boundary conditions that $|\psi|$ is zero at the wall as well as on the surface ψ can be solved. When this formalism is

applied to helium films it appears that starting from a certain thickness d_c no solution $\psi \neq 0$ can be found for films thinner than d_c, so that the film ceases to be superfluid. As it is a macroscopic theory, it is only valid for dimensions much larger than the interatomic distance, *i.e.* for temperatures not too far from the bulk-helium λ-point. The final result for the shift of the λ-point is $\Delta T = 2 \times 10^{-14}/d^2$. For films thicker than 15 Å indeed a d^{-2} behaviour is found but the theoretical values are a factor 3 too small. Perhaps a better agreement can be obtained by introducing into the calculations the Van der Waals forces between the helium and the wall.

7. *³He–⁴He mixtures.* In the apparatus we used before to measure the heat conductivity coefficient of gaseous ³He and ⁴He[11]) and which was schematically shown in fig. 2, the onset of superfluidity in films of adsorbed ³He-⁴He mixtures was studied. As already mentioned in section 2 this apparatus was not suited to measure critical heat currents because of the fact that the diameter of the walls was not uniform. Therefore, the temperature difference between the two horizontal plates was measured at a constant heat input in the upper plate as a function of the pressure in the apparatus.
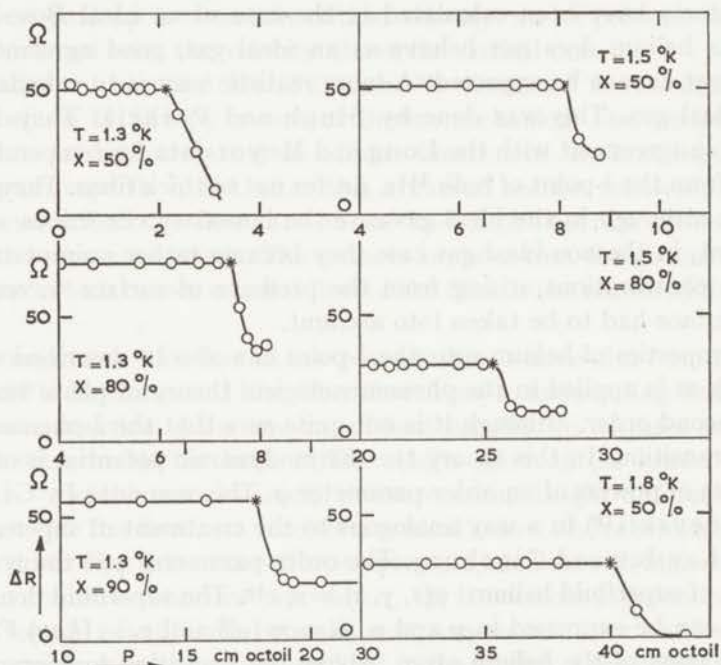

Fig. 9. The dependence of the change in temperature of the upper plate on the pressure at a constant heat input, expressed in the change in resistance of the thermometer, ΔR, for various temperatures and gas concentrations X

     ○   measured points
     ✳   onset of superfluidity

36

Below the pressure where the superfluidity sets in, the temperature difference remains almost constant, the conductivity being pressure independent as long as no mean free path effects take place. But as soon as the film becomes superfluid the temperature difference drops. In fig. 9 this behaviour is shown for various concentrations and temperatures. Along the vertical axis we plotted the temperature difference expressed in the change in resistance of the carbon thermometer. It corresponds to a few millidegrees.

We examined three gas mixtures in which the concentrations of the ^{3}He at room temperature were respectively 50%, 80% and 90%.

As a consequence of selective adsorption neither the concentration of the film nor that of the vapour phase have these values. However, if one knows the total amount of ^{3}He and ^{4}He in the apparatus and the amount that is adsorbed, and if one assumes – we cannot prove it – that for the equilibrium of an unsaturated film and its vapour the same concentration ratio's are valid as for the liquid-vapour equilibrium, then the concentration of the films can be calculated, although no high precision can be claimed.

As an example we give here the calculation for a 50% mixture at 1.3°K. Let the total input be A cm^3 N.T.P. Then we can apply the following scheme:

	^{3}He	^{4}He	total
input (cm^3 N.T.P.)	b	b	$2b = A$
adsorbed ,,	p	q	$p + q = Z$
in gaseous state ,,	$b - p$	$b - q$	

For the concentration of the gaseous phase X_g this leads to the equation

$$X_g = \frac{b - p}{2b - q - p} = \frac{0.5A - p}{A - Z}.$$

A and Z can be measured.

Now an iteration method gives the concentration of the film.

A bulk liquid mixture in equilibrium with a vapour phase of 50% ^{3}He should have a concentration $X_1 = 2\%$[20]). Following our assumption, which is also based on experiments of Inghram, Meyer and Long[21]), the concentration of the film X_f would also be 2%. So in first approximation $p = 0.02 Z$. At the pressure where the superfluidity sets in, $A = 4$ cm^3 and $Z = 0.6$ cm^3. This leads to $X_g = 60\%$, which corresponds to a X_1 value of 3%. Substitition of $p = 0.03 Z$ leads to $X_g = 58\%$ and $X_f = 2.5\%$. The value of $X_g = 58\%$ is in agreement with the measurements of the heat conductivity coefficient of a mixture, that had a concentration of 50% at room temperature. When one substitutes the result, as published in reference 11, in the theoretical derivation of Cohen $e.a.$[22]) this leads to a corresponding concentration of about 60%, which is within the accuracy of our calculation given above. Similar calculations have been made for the other concentrations and temperatures to derive X_f.

The total amount of gas that was used was measured in a pipet system of known volume at room temperature by measuring the pressure on an oil manometer filled with octoil-S. The adsorbed quantity Z was calculated from the final pressure of the gas after expansion into the apparatus. The volume of the apparatus was calibrated by expansion of a known quantity of helium gas from a pipet to the apparatus at room temperature as well as at the normal boiling point of liquid nitrogen. It appeared to be 6.37 ± 0.05 cm³. Because of this large volume an important correction had to be made for the non-ideality of the gas at low temperatures. To do this we used the values of the B-coefficients Keller *e.a.*[23]) calculated for pure ⁴He and ³He gas and their values for B_{34}. In the usual way we interpolated between these
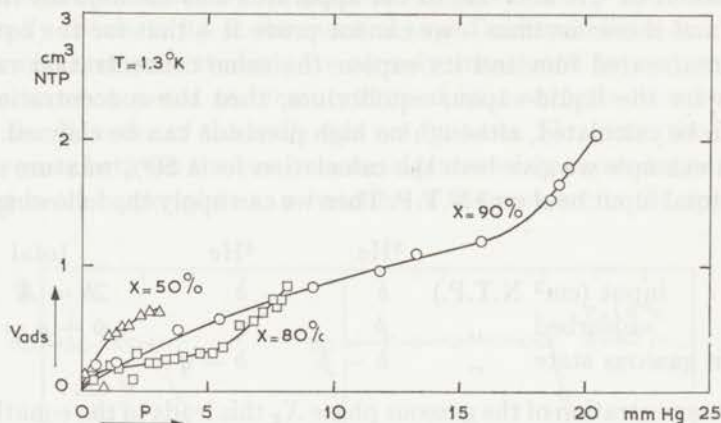

Fig. 10. Adsorption isotherms.
The adsorbed amount, expressed in cm³ *N.T.P. versus P* for different gas concentrations at $T = 1.3°K$.

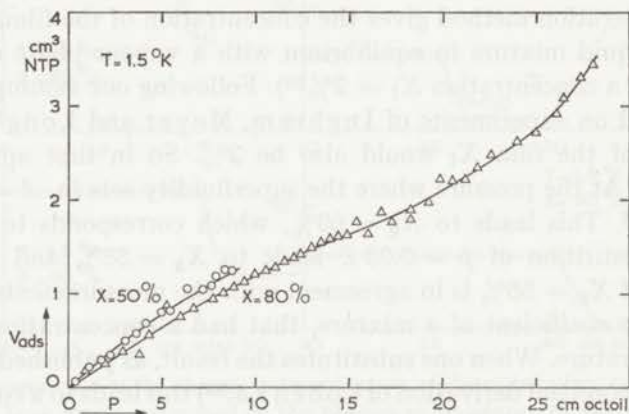Fig. 11. Adsorption isotherms.
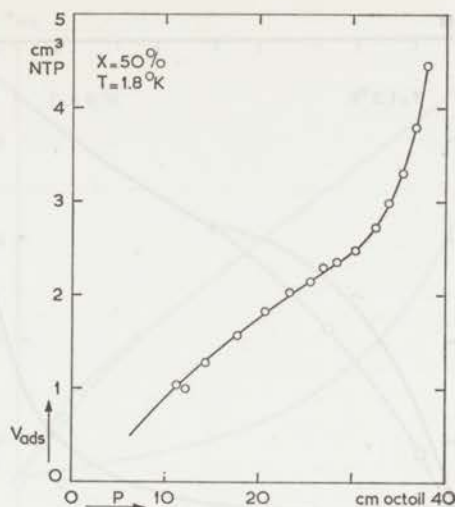The adsorbed amount, expressed in cm³ N.T.P., *versus P* for different gas concentrations at $T = 1.5°K$.

Fig. 12. Adsorption isotherms.
The adsorbed amount, expressed in cm³ N.T.P. *versus* P for one gas
concentration at $T = 1.8°K$.

to get the B-coefficients of our ³He–⁴He mixtures. The adsorption isotherms
we measured are plotted in the figures 10, 11 and 12. We plotted the adsorbed
volume against the pressure P, not against P/P^0 because P^0 is not constant
during one series of measurements as the concentrations change with the
pressure. P is expressed in mm Hg or in cm octoil-S ($\rho_{Hg} = 13.85\ \rho$ octoil-S)
One sees that at low values of P the adsorbed amount is a linear function of
the pressure.

This might indicate that the gas volume is larger than calculated. The
extra volume calculated from the slope of the isotherms would be about
1 cm³ at room temperature, which is in contrast with the accuracy of the
calibration we made. Moreover, the amount of ⁴He that has to be withdrawn
from the total input to enrich the 50% mixture to a 58% mixture is of the
same order of magnitude as follows from our adsorption measurements.

TABLE IV

$T = 1.3°K$		$T = 1.5°K$		$T = 1.82°K$	
X_f	$(P/P_3^0)_c$	X_f	$(P/P_3^0)_c$	X_f	$(P/P_3^0)_c$
0.02	0.055	0.045	0.105	0.09	0.24
0.08	0.175	0.20	0.33		
0.26	0.425				

The results are given in table IV.

In the figures 13, 14 and 15 the onset of the superfluidity is given in
reduced diagrams. The vertical co-ordinate is P/P_3^0, where P is again the
pressure of the gas, and P_3^0 the saturated vapour pressure of liquid ³He at

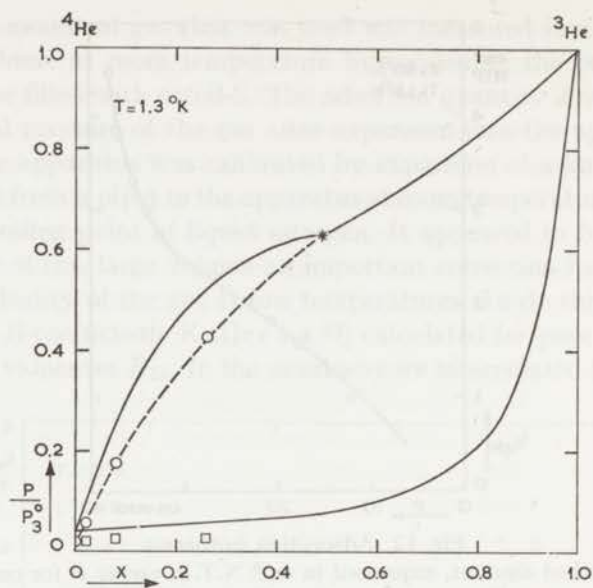Fig. 13. Reduced phase diagram at $T = 1.3°$K.
- - - line of the onset of superfluidity.
* λ-point of the bulk mixture
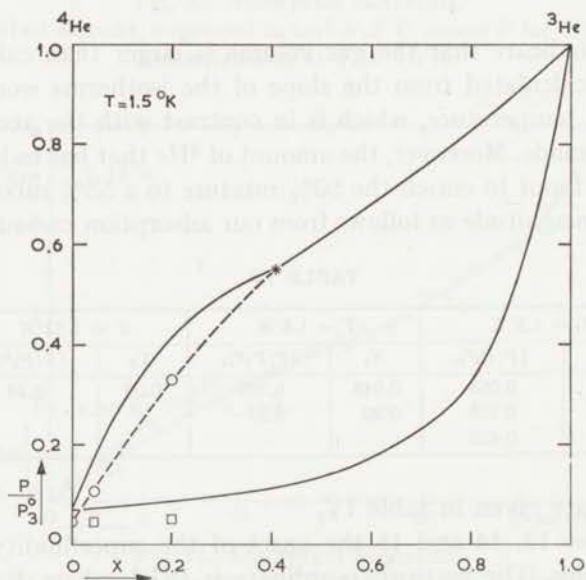○ measured values of $(P/P_3^0)_c$.
□ partial ^{4}He pressure

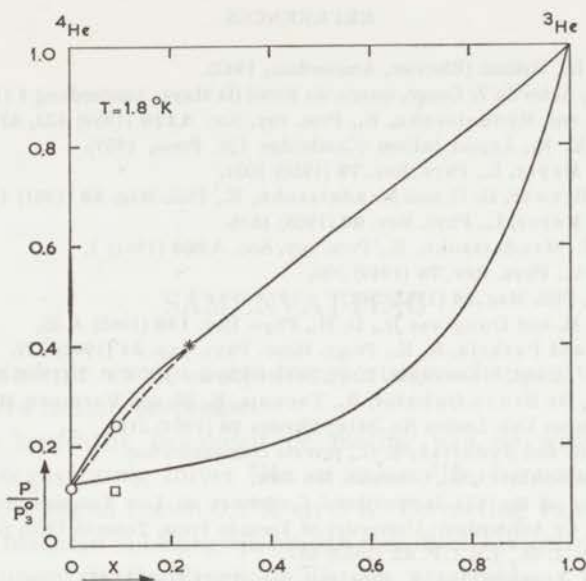
Fig. 14. Reduced phase diagram at $T = 1.5°$K symbols see fig. 13

Fig. 15. Reduced phase diagram at $T = 1.8°K$ symbols see fig. 1.3

the same temperature. The horizontal co-ordinate is the ^{3}He concentration of the film. The drawn lines are the boiling and dew lines of the liquid mixtures [20]. The dotted lines give the onset of superfluidity in the unsaturated films. At the $X = 0$ side they end at the measured pressure of the onset of superfluidity in pure ^{4}He films. At the other side they are extrapolated to the λ-point in the bulk liquid mixtures. Also the partial ^{4}He pressure P_4 where superfluidity sets in expressed in terms of P_4/P_3^0 is plotted. This appears to be a horizontal line. As, however, the vapour curve is almost horizontal in this region, this is not surprising.

REFERENCES

1) Keesom, W. H., Helium (Elsevier, Amsterdam, 1942).
2) Rollin, B. V., Actes du 7e Congr. intern. du Froid (la Haye, Amsterdam) **1** (1936) 187.
3) Daunt, J. G. and Mendelssohn, K., Proc. roy. Soc. **A170** (1939) 423, 439.
4) see Atkins, K. R., Liquid helium (Cambridge Un. Press, 1959).
5) Long, E. and Meyer, L., Phys. Rev. **79** (1950) 1031.
6) Bowers, R., Brewer, D. F. and Mendelssohn, K., Phil. Mag. **42** (1951) 1445.
7) Long, E. and Meyer, L., Phys. Rev. **98** (1955) 1616.
8) Brewer, D. F., Mendelssohn, K., Proc. roy. Soc. **A260** (1961) 1.
9) Osborne, M. F., Phys. Rev. **76** (1949) 396,
   Ziman, J. M., Phil. Mag. **44** (1953) 548,
   Khorana, B. M. and Douglass Jr., D. H., Phys. Rev. **138** (1965) A 35,
   Singh, A. D. and Pathria, R. K., Progr. theor. Phys. Jap. **24** (1960) 229.
10) Ginzburg, V. L. and Pitaevskii, L. P., Soviet Physics J.E.T.P. **7** (1958) 858.
11) Fokkens, K., De Bruyn Ouboter, R., Taconis, K. W. and Vermeer, Miss W., Commun. Kamerlingh Onnes Lab. Leiden No. 341*a*; Physica **30** (1964) 2153.
12) Roberts, T. R. and Sydoriak, S. G., private communication.
13) Weber, S. and Schmidt, G., Commun. No. 246*c*.
14) see Proceedings of the VII International Conference on Low Temperature Physics (North Holland Publ. Cy Amsterdam; University of Toronto Press, Toronto 1960) p. 466–487.
15) Khalatnikov, I. M., J.E.T.P. **22** (1952) 687.
16) Fairbank, H. A. and Wilks, J., Proc. roy. Soc. **A231** (1958) 548.
17) Kuang, Wey Yen, Soviet Physics J.E.T.P. **15** (1962) 6352.
18) Long, E. and Meyer, L., Adv. in Phys. **2** (1953) 1.
19) Frederikse, H. P. R., Thesis, Leiden 1950.
    Frederikse, H. P. R. and Gorter, C. J., Leiden Commun. No. 278*e*; Physica **15** (1949) 860.
20) Roberts, T. R. and Sydoriak, S. G., Phys. Rev. **118** (1960) 901.
21) Inghram, M. G., Meyer, L. and Long, E., Phys. Rev. **39** (1955) 1453.
22) Cohen, E. G. D., Offerhaus, M. J. and De Boer, J., Physica **20** (1954) 501.
23) Kilpatrick, J. E., Keller, W. E. and Hammel, E. F., Phys. Rev. **97** (1955) 9 and Phys. Rev. **94** (1954) 103.
24) Atkins, K. R., Proc. roy. Soc. **A203** (1950) 240.
25) Chandrasekhar, B. S. and Mendelssohn, K., Proc. Phys. Soc. **A68** (1955) 857.
26) Seki, H., Phys. Rev. **128** (1962) 502.
27) Van Alphen, W. M., to be published.
28) Wansink, D. N. and Taconis, K. W., Commun. Leiden No. 306*b*; Physica **23** (1957) 273.
29) Brewer, D. F., Symonds, A. J. and Thomson, A. L., Phys. Rev. Letters **15** (1965) 182.
30) Goble, D. F. and Trainor, L. E. H., Phys. Letters **18** (1965) 122.

SAMENVATTING

In dit proefschrift worden enige transporteigenschappen van gasvormig en geadsorbeerd helium besproken.

Het eerste hoofdstuk behandelt de meting van de warmtegeleidingscoëfficiënt van gasvormig zuiver ^{3}He en zuiver ^{4}He, benevens die van een 50% ^{3}He–^{4}He mengsel tussen 0,5°K en 3°K. De meting van deze warmtegeleidingscoëfficiënten is belangrijk omdat zeer duidelijk quanteuze effecten optreden, wanneer de De Broglie golflengte vergelijkbaar wordt met de molecuuldiameter. Bovendien zullen bij een botsing van twee identieke deeltjes de golffuncties gesymmetriseerd moeten worden, zodat de transportgrootheden afhangen van de statistiek, waaraan de deeltjes gehoorzamen, nl. Fermi-Dirac statistiek voor ^{3}He en Bose-Einstein statistiek voor ^{4}He.

De warmtegeleiding wordt gemeten tussen twee horizontale evenwijdige platen. De bovenplaat is omgeven door een schutring, die dient om het warmtetransport langs de wand te elimineren. De bovenplaat en de schutring kunnen samen op en neer bewogen worden, waardoor de plaatafstand gevarieerd kan worden. De warmtegeleidingscoëfficiënt wordt bepaald door het temperatuurverschil tussen boven- en onderplaat te meten, als functie van de aan de bovenplaat toegevoerde warmte, wanneer de schutring op dezelfde temperatuur is gestookt. Door bij verschillende plaatafstanden te meten kan worden gecorrigeerd voor temperatuursprongen aan het plaatoppervlak. Bovendien kan gecontroleerd worden of convectie optreedt. Uit het feit dat de warmteweerstand evenredig bleek te zijn met de plaatafstand, bleek dat het apparaat convectie-vrij was.

De resultaten zijn, wat betreft de pure componenten, in goede overeenstemming met theoretische berekeningen van Keller e.a., Buckingham en Scriven en van Mason e.a. De resultaten bij het 50% mengsel wijken nogal af van de berekende waarde van Cohen e.a. De reden hiervan is, dat door de selectieve adsorptie aan de wand de concentratie een functie van de temperatuur wordt, wanneer men van één mengsel uitgaat.

In hoofdstuk II worden metingen van het massatransport door onverzadigde ^{4}He films onder invloed van een toegevoerde warmtestroom beschreven als functie van de druk boven de film in het temperatuurgebied tussen 0,8°K en 1,7°K. De critische druk, die nodig is om een film te adsor-

beren, die superfluide is, werd bepaald. Doordat de adsorptieisothermen onvoldoende bekend zijn, vooral beneden 1,3°K, kan de dikte van de film niet exact worden opgegeven. Als relevante grootheid gebruiken we de verhouding tussen de druk en de verzadigde dampspanning. De critische waarde hiervan is bij 0.8°K reeds gezakt tot ongeveer 0.05. Boven 1,3°K is goede overeenstemming bereikt met eerdere metingen van Long en Meyer en van Brewer en Mendelssohn. Tenslotte werd de minimale druk bepaald, die bij gegeven temperatuur en concentratie moet heersen boven een geadsorbeerde film van een ^{3}He–^{4}He mengsel, opdat ook deze films superfluide worden. De resultaten worden weergegeven in gereduceerde fasediagrammen. Om de concentraties van de films te kunnen berekenen werden voor de gebruikte gasmengsels adsorptieisothermen opgenomen.

STELLINGEN

I

Meting van de thermodiffusiecoëfficient in gasvormige ^{3}He–^{4}He mengsels bij zeer lage temperaturen is zeer bezwaarlijk door de druk- en temperatuurafhankelijkheid van de concentratieverhouding tussen de geadsorbeerde film en de gasfase.

II

Bij experimenten met helium, waarbij nauwe toevoerleidingen noodzakelijk zijn om het schadelijke volume te beperken, moet rekening worden gehouden met de invloed, die het kruipen van heliumfilms heeft op eventuele drukmetingen.

III

De door Park gegeven verklaring van de verschijnselen, die optreden bij de beweging van fluxbuizen in een supergeleider van het eerste type, is onvolledig.

Park, J. G., Phys. Letters **20** (1966) 346.

IV

De verklaring van het verschil in viscositeit tussen HD en D$_2$, die Diller en Mason geven door het verschil in potentiaal-parameters te schatten uit het verschil in nulpuntsenergie, is onjuist.

Diller, D. E. en Mason, E. A., J. Chem. Phys. **44** (1966) 2604.

V

Bij de voorstellen van Lovejoy tot uitbreiding van de internationale temperatuurschaal tot 12°K is onvoldoende aandacht besteed aan de reproduceerbaarheid van platina-weerstandsthermometers.

VI

Het is te betreuren, dat Pippard heeft gemeend zijn boek "The Elements

of Classical Thermodynamics" te verbeteren door in de laatste druk een beschouwing op te nemen over de derde hoofdwet der thermodynamica in verband met het gedrag van ^{3}He–^{4}He mengsels.

Pippard, A. B., "The Elements of Classical Thermodynamics", 4e druk, 1964, pag. 129.

VII

Het door Pankove gevonden "nieuw effect in supergeleidende contacten" is op eenvoudige wijze te verklaren.

Pankove, J. I., Phys. Letters **21** (1966) 406.

VIII

De afleiding, die Zimmerman geeft voor de vergelijking, die het analogon van het a–c Josephson-effect in helium beschrijft, is onvolledig.

Zimmerman, W., Phys. Rev. Letters **14** (1965) 976.

IX

Opdat een werkcollege resultaten afwerpt, is het van belang, dat er discussies ontstaan tussen de assistent en de studenten.

X

Het is gewenst, dat in de scholen voor V.H.M.O. de activiteiten van de schoolmusicus zich ook uitstrekken over de gebieden van geschiedenis, litteratuur, beeldende kunsten en natuurkunde, om de culturele samenhang van de muziek met genoemde gebieden te beklemtonen.

K. Fokkens, 21 september 1966

of Classical Thermodynamics" te verbeteren door in de laatste druk een beschouwing op te nemen over de derde hoofdwet der thermodynamica in verband met het gedrag van ^{4}He–^{3}He mengsels.

Klippard, A. B., "The Elements of Classical Thermodynamics", 4e druk, 1964, pag. 123.

VII

Het door Pankove gevonden "nieuwe effect in supergeleidende contacten" is op eenvoudige wijze te verklaren.

Pankove, J. I., Phys. Letters 21 (1966) 40.

VIII

De afleiding, die Zimmerman geeft voor de vergelijking, die het analogon van het a-c Josephson-effect in helium beschrijft, is onvolledig.

Zimmerman, W., Phys. Rev. Letters 14 (1965) 976.

IX

Opdat een verrassende resultaten alwijst, is het van belang, dat er discussie ontstaat tussen de assistent en de studenten.

X

Het is gewenst, dat in de scholen voor V.H.M.O. de activiteiten van de schoolmusea zich ook uitstrekken over de gebieden van geschiedenis, litteratuur, beeldende kunsten en natuurkunde, om de culturele samenhang van de mensch met genoemde gebieden te belichten.

E. Tieckeus, 31 september 1966.